Thermochimica Acta, 29 (1979) 1–39

A review

Modern low-temperature calorimetry

E. GMELIN
Max-Planck-Institut für Festkörperforschung, 7000 Stuttgart 80 (Federal Republic of Germany)
(Received 16 March 1978)

CONTENTS

ABSTRACT

A review is presented of recent trends, technical developments and applications of low-temperature calorimetry ($0.05 < T < 300$ K) in the field of solid state research.

After some historical remarks, the importance of low-temperature calorimetry and its application is shown by several selected results. Adiabatic and non-adiabatic methods are then reviewed with emphasis on automatic data acquisition, computer-controlled processing and data evaluation and on recent progress in experimental techniques and newly developed methods. A fully automated adiabatic Nernst-type calorimeter and a new type of differential calorimetric measurement (for very low temperatures) are described in more detail. Special processes to determine the heat capacity of samples under extreme conditions, such as very small (milligram) samples, very low temperatures ($T < 1$ K) or high magnetic fields, are discussed. Throughout the review, emphasis is given to what has been achieved in recent years and the areas where problems still remain. No attempt is made to give a comprehensive description of all experimental work in the field of low-temperature calorimetry.

1. INTRODUCTION

1.1 Historical

The "specific heat" is one of the important basic parameters in solid state research. Therefore low-temperature heat capacity data have today a fundamental significance in physics, chemistry and technical thermodynamics as well as in biology and medicine. The concept of low-temperature calorimetry was developed by Gaede[1] in 1902, and especially by Nernst[2] and Eucken[3] in 1910, introducing the modern low-temperature adiabatic, better described as quasi-adiabatic, calorimeter. Precise calorimetric values at liquid helium temperatures started in 1922 with the development of a very sensitive phosphor-bronze thermometer by Keesom and Van den Ende[4] and with the introduction of refined low-temperature calorimetric techniques introduced by Southard and Andrews[5]. Since that time, the experimental methods have continuously improved and our knowledge and understanding of the specific heats of solids, liquids and gases at low temperatures have increased enormously.

In the decade from 1955 to 1965, a new area of high precision calorimetry has been entered, enabling an accuracy with errors less than 0.5% instead of 1–2% to be achieved, and with a temperature resolution of 10^{-6} K or better below 20 K. Many of these calorimeters may be operated over a wide temperature range (1.5–100 K, or even

up to 300 K) and are supplied with one or more automatic temperature controllers for the temperature regulation of the radiation shields. Reviews on these developments and the state of the technology have been given by Cole and Hutchens, Hill, and by Keesom and Pearlmann[6]. A very detailed survey of low-temperature calorimetry and related problems was presented by Westrum et al.[7] in 1968.

1.2 Recent trends in low-temperature calorimetry

In spite of this progress, several difficulties of low-temperature heat capacity measurement still persist, mainly the tedious and monotonous methods used to record, analyse and evaluate the experimental data. Furthermore, special demands such as measurement of very small samples, taking data at high pressure, at extremely low temperatures or in high magnetic fields, require knowledge and more experience in non-adiabatic methods, their significance and computing methods as well as the development of new special techniques. The most important advances in the field of low-temperature calorimetry made in this decade are the following.

(1) Computer-aided data acquisition, computer-controlled processing and data evaluation[8-19]. The advantages of the application of computers or microprocessors are easy to understand. They include increased precision by digital technique; the possibility of fully automated real time processing of the experiment; easy data handling by immediate data enregistration and transfer for further interpretation (data-fitting, integration, elimination of incorrect values, extraction of anomalies); immediate correction of data by pre-defined programs for non-adiabatic condition, addenda heat capacity subtraction, data reduction to unit mole-number, and rapid or even real-time data evaluation.

(2) Development of new and specialized technique as, for example; (a) Measurements of small heat capacities ($C < 10^{-6}$ J/K), small samples having only a few milligrams of mass ["AC-techniques" of Sullivan and Seidel[20]; "relaxation-time method" of Bachmann et al.[21]; differential relaxation-time measurement (see Sect. 5.2)]. (b) Rapid measurements, mainly used for rough orientational data or for simultaneous measurements of thermal conductivity λ and heat capacity C_p (continuous heating method; differential scanning calorimetry; measurement of thermal diffusivity $D = \lambda/C_p$). (c) Considerable effort has also been directed by several authors to the determination of the heat capacities under extreme conditions, such as very high magnetic fields (development of B-field independent thermometers[22] and research on the magnetic field dependence of thermometers[23]) and pressures[28-32], and to more or less exotic, but quite interesting, problems which have also been studied with success, e.g. samples with extremely low thermal diffusivity[13]; samples of high radioactivity[33]; controlled heating of sample and shield by light, especially by laser light[34, 81] or by electron beams[35]; and the large field of techniques for the investigation of gases and liquids, which solidify at low temperatures (e.g. argon, helium-4 and helium-3).

Significant improvements concerning the precision of data must be attributed to modern electronics and to more sensitive, better reproducible, commercially

available and relatively low-priced semiconductor-thermometers[36] for the low-temperature region.

This paper is intended to illustrate the importance of low-temperature calorimetry and review the above-listed technical developments and problems. The discussion will be neither comprehensive nor complete; this contribution aims at pointing out only some of the essential features of low-temperature calorimetry; for more detailed information the reader is referred to the indicated original literature. The importance and vitality of the whole field of low-temperature calorimetry is elucidated by several selected recent results in Sect. 2. The following part (Sect. 3) describes the basic problems of calorimetry at low temperatures. Sections 4–6 review the different adiabatic and non-adiabatic methods as well as other special experimental procedures. The recent progress in calorimetric technique is demonstrated by the description of a fully automated computer-controlled adiabatic calorimeter of the Nernst type for the temperature range 0.3–350 K[19] and by the presentation of a new calorimetric method for the study of milligram samples below 1 K.

2. APPLICATION OF LOW-TEMPERATURE CALORIMETRY

The total heat capacity of a solid is defined by

$$C_{x,y\ldots} = \lim_{T\to 0}\left(\frac{\mathrm{d}Q}{\mathrm{d}T}\right)_{x,y\ldots}$$

where, by convention, $C_{x,y\ldots}$ refers to the specific heat per gram-molecule with the parameters $x, y \cdots$ being held constant. Hence, during experiments for which the pressure p is kept constant, the corresponding heat capacity is defined as $C_p = (\mathrm{d}Q/\mathrm{d}T)_p = T(\partial S/\partial T)_p$* in the case of solids, to which we restrict ourselves here.

The specific heat reflects the distribution of the energy levels of a physical system. The ensemble of energy levels, expressed by the density of states, leads directly to the partition function from which the heat content is derived by differentiation with respect to the temperature. The inverse of this procedure, however — to yield information on the level structure by experimental C_p data — is not possible even for the most accurate measurements. Therefore, one must attempt to find a model for the energy-level system which reproduces the experimental specific heat data. This strong connection between energy and specific heat is, at the same time, the strength and the weakness of specific heat measurements. Consequently, the C_p measurements do not, in general, elucidate the detailed structure of a special physical system. Instead, by this type of experiment, the overall feature of the energetic contributions is given and a general knowledge of the different types of contributing systems, i.e. phonons, spins, lattice-crystallographic transitions, is obtained. Therefore, specific heat experiments are a powerful tool in many areas of physics and chemistry:

* Q is the energy supplied to sample and S is the entropy.

thermodynamic studies, electronic, vibrational and magnetic research, crystal structural transition research or investigation of cooperative phenomena.

The example of the parameter "characteristic Debye temperature", θ, present in nearly every branch of solid state research, gives evidence to the importance of C_p data. Furthermore, the drastic reduction in specific heat at low temperatures by a factor of 10^4 to 10^7 with respect to room temperature underlines the tremendous significance of knowledge of C_p data for cryogenic application. Finally, it should be noted that in view of the third law of thermodynamics, the ratio of two absolute temperatures T_1/T_2 is more important than their difference $T_1 - T_2$. Consequently, from a fundamental point of view, a temperature reduction from room temperature to 30 K is as significant as cooling from 3 to 0.3 K. In practice, a linear temperature scale is used, but it must be emphasized that the temperature scale at low temperatures should be regarded logarithmically.

In the following, we present a small selection of representative specific heat curves in order to point out how, in spite of the integral character of the parameter C_p, heat capacity measurements are of basic significance in solid state physics. Therefore we restrict ourselves to a general description of the results, excluding any detailed discussion of the theoretical background. For more details, the reader is referred to the original literature, to text books, or to the excellent survey of Gopal[38].

2.1 Basic thermodynamic functions

Physical chemistry needs measurements of the highest practical accuracy for the evaluation of fundamental thermodynamic functions such as entropy, S, enthalpy, H, and Gibbs free-energy, G. These measurements have to be performed from the lowest temperatures, which means about 1.5 K (pumped liquid helium-4), up to room temperatures, since very frequently the most important contributions originate from the low-temperature region (1–100 K), that is, large C_p values are associated with zero-point entropy or any anomalies in the specific heat, examples of which will be discussed in the following.

The importance of a knowledge of S, H and G in understanding reactions is worth mentioning in more detail. The disappearance of the specific heat as $T \to 0$, following the Nernst-law, is of fundamental significance, because it enables the experimentalist to use the absolute zero point of temperature as a reference for all thermodynamic calculations without any undetermined constant. Furthermore, in the field of physical chemistry, experimental values for certain selected materials, i.e. copper, Cu, or alumina, Al_2O_3, are currently used as standard substances for comparison and for elimination of systematic errors in the absolute temperature scale, used in connection with other experiments[39, 40].

Figure 1 shows the specific heat of the ionic conductor TeI in a C_p vs. T plot between 1.5 and 320 K[41]. The plot shows the typical, well-known phonon contribution represented by the Debye function [θ_0(TeI) = 135 K]. At high temperatures ($T >$ 150 K), the expected constant specific heat exceeds the Dulong–Petit value for diatomic materials. The constant linear increase of C_p (thick line in Fig. 1) is due to a

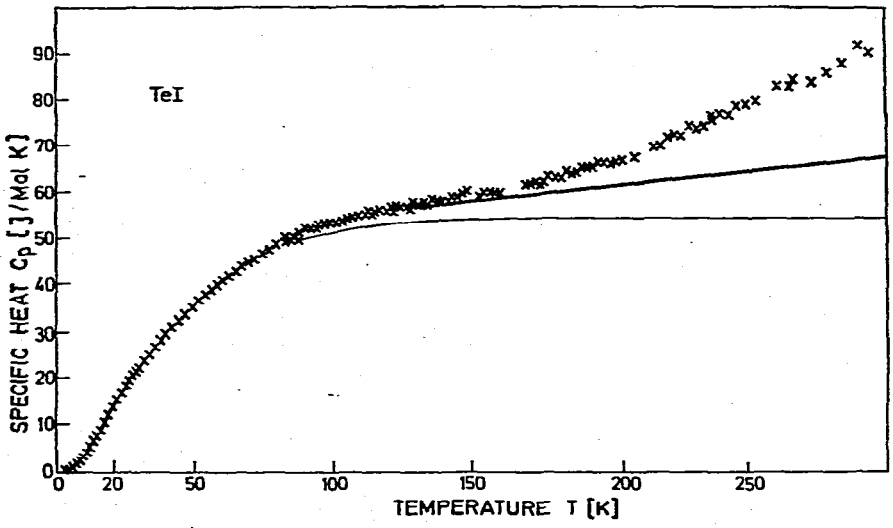

Fig. 1. Specific heat C_p of TeI as a function of temperature T, ×, experimental values, reduced to gram-mole unit; ——, Debye law, calculated with θ_0 (TeI) = 135 K; ——, anharmonic lattice vibrational contribution included by extrapolation from the temperature range 40 K < T < 100 K.

general feature of the heat capacity of solids: the anharmonicity of lattice vibrations. A further, rather small, exponentially rising behavior of C_p (TeI) above 220 K can be explained by the strongly increasing diffusivity of ions in this ionic conductor[41]. The integration of the thermodynamic functions S, ΔH and G yields the standard values at °C:

S (298,15 K) = 109 JK^{-2} $mole^{-1}$
ΔH (298,15 K) = 12.7 kJK^{-1} $mole^{-1}$

These experimental results are in excellent agreement with values deduced from electromotive force measurements (e.m.f.) of electrochemical cells of the type AgI | TeI | Ag.

In this special case, the direct specific heat data prove the correctness of assumptions made for the indirect calculation of S from e.m.f. measurements; consequently, the result is of fundamental importance for the interpretation of further e.m.f. data on ionic conductors[41].

2.2 Vibrational and electronic properties of solids (electrons and phonons)

In the liquid helium range (1.2–4.2 K), the vibrational contribution to the specific heat C_l is proportional to T^3 corresponding to Debye's theory, while the contribution of the electrons C_{el} obeys a simple T law. Therefore, in the absence of any further anomalous contribution the low-temperature heat capacity of solids is given by

$$C_p = C_{el} + C_l = \gamma T + \alpha(T/\theta)^3 \qquad (1)$$

with the following meaning.

(a) The free electron term γ[42, 43] includes the density of state $n(E)$ at the

Fermi energy and the effective mass, m_{eff}. These are essential experimental parameters needed for comparison with band structure calculations.

(b) The low-temperature limiting lattice term $(\alpha/\theta^3)T^3$ with $\alpha = 1944.6$ mJ K^{-1} Mol^{-1} yields the Debye temperature θ_0 at 0 K. The lattice specific heat, C_l, has a pure cubic temperature dependence with less than 1% deviation from Debye's function only below $T < (\theta_0/50)$; at high temperatures the exact Debye function must be taken to represent C_l. The data may be compared with those from elastic constant measurements. A representation C_p/T vs. T^2.

$$C/T = \gamma + (\alpha/\theta_0^3)T^2 \tag{2}$$

enables γ and θ_0 to be extracted from the ordinate distance and slope of eqn. (2).

An example is shown in Fig. 2. Therein the specific heat of the ternary semiconducting material $AuTe_2I$[44] is plotted as C_p/T vs. T^2. The composition exhibits low θ_0 value and, due to the semiconducting properties, a far smaller γ value than observed for metals. Consequently, the measurement has to be performed at "very low" temperatures, down to 0.4 K as can be seen from Fig. 2.

The rather low Debye temperature $\theta_0(AuTe_2I) = 139$ K obtained characterizes the layer structure of $AuTe_2I$; the experimental value of the electronic γ term in connection with the effective mass data which has been derived from Shubnikov–de Haas experiments[103] yield $n(E) = 2.10^{20}$ electrons cm^{-3} in accordance with the number of free carriers obtained from the computation of Hall effect measurements[103].

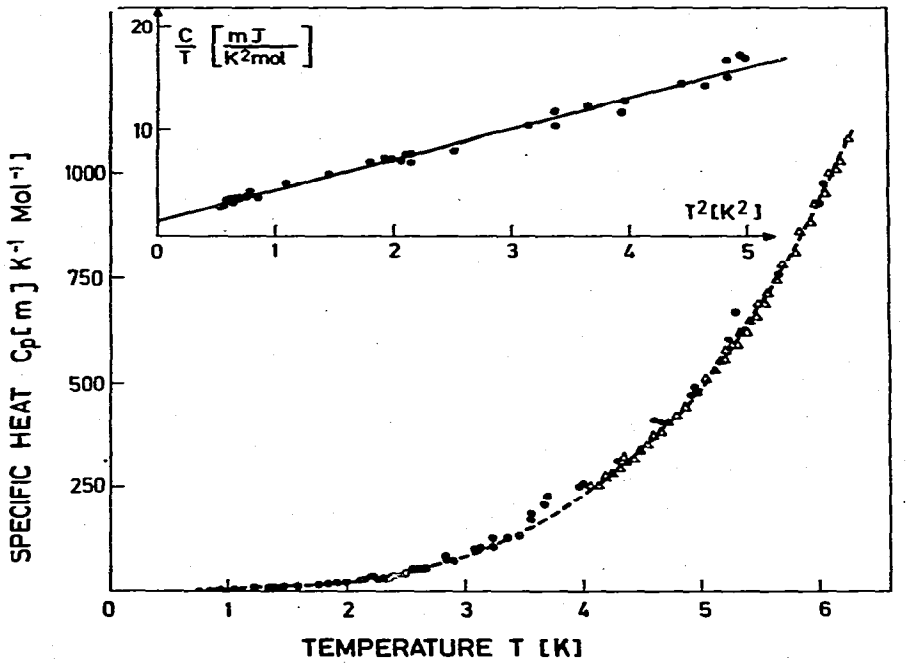

Fig. 2. Specific heat C_p of $AuTe_2I$ as a function of temperature T. Insert figure represents C_p/T as T^2 to determine the electronic contribution γ and the Debye temperature θ_0 from the ordinate distance and slope, respectively: θ_0 (AuTeI) = 139 K; $\gamma = 1.40$ mJ/mole K^2. • • •, Experimental data taken by the "relaxation-time method"[44] within a helium-3 cryostat (temperature range 0.4 K < T < 10 K); △, data measured with an adiabatic, automatized Nernst calorimeter[19].

It is fairly well-known that, due to the discrete structure of matter, the realistic phonon spectra are altered radically compared with the ν^2 behavior in the Debye model; alterations occur at temperatures above 10 K and therefore the corresponding "Debye characteristic temperature", $\theta(T)$, becomes temperature-dependent. The specific heat is very often expressed by a function $\theta = \theta(T)^*$, which reveals the drastic variation of the phonon density of states compared with the ν^2 behavior. This type of representation gives the possibility of obtaining the real phonon spectra at low temperatures.

As an example, the lattice specific heat of "high-temperature" superconducting TaC is reduced by the Debye function to a $\theta(T)$ vs. T curve, plotted in Fig. 3. Note that, prior to the calculation of $\theta(T)$, the electronic γ term has been subtracted by

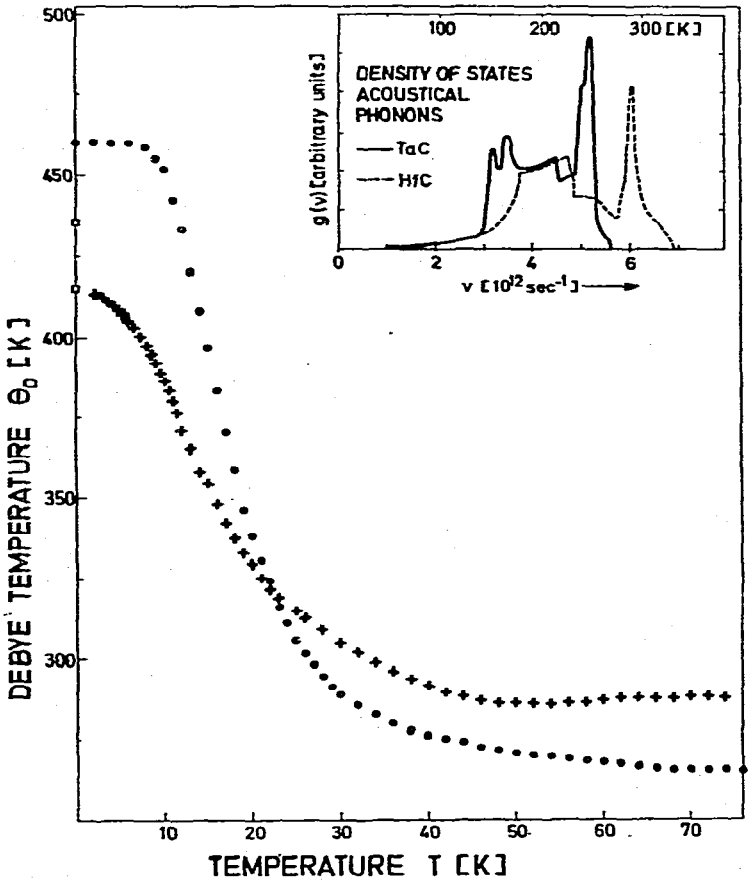

Fig. 3. Temperature dependence of Debye-temperature $\theta(T)$ of TaC and HfC as a function of temperature T[45]. +, Experimental results on HfC; • • • experimental data of TaC. The insert gives the phonon spectra of HfC and TaC: the steep increase of the phonon density of states at the low-frequency side can be fitted only by an additional exponential term (Einstein anomaly with ω_E):

$$C_p = \gamma T + (\alpha/\theta_0^3)\, T^3 + A \exp(\hbar\omega_E/kT);\ T \ll T_E = \frac{\hbar\omega}{K}$$

* The reader should not forget that θ is a constant in the Debye theory.

the procedure shown in Fig. 2. The overall decrease of $\theta(T)$ is a common feature of most solids. However, the outstanding characteristic of the present curve for TaC (points in Fig. 3) is the fact, that a fit of the $C_p(T)$ or $\theta(T)$ curve in the temperature range 20–50 K, requires an additional exponential term

$$C_p = \gamma T + (\alpha/\theta_0^3)T^3 + \beta\exp(\hbar\omega_E/KT)$$

This is in contrast to the usual additional T^5 and T^7 terms in the normal representation of C_p vs. T in the case of the non-superconducting materials, e.g. HfC (points + in Fig. 3).

The exponential increase of C_p(TaC) [or decrease of $\theta(T)$] is produced by a low-lying phonon anomaly (having a high phonon density of states) at the frequency ω_E. This phonon anomaly may be described by an Einstein term with the characteristic frequency ω_E which gives an additional contribution to the specific heat, and which causes the exponential increase of C_p(TaC) at sufficiently low temperatures[45]. It turned out that such phonon anomalies play a vital role in determining the strength and characteristics of the electron–phonon interaction, which itself is responsible for the appearance of superconductivity. Instead of neutron dispersion experiments (requiring single crystals which are not always available) specific heat experiments here opened a new way to determine the frequency of phonon anomalies in high-temperature superconductors, using simple hot-pressed sintered materials. In this way, the entire series of transition metal carbides and nitrides[46] has been investigated to elucidate the role of electron–phonon interaction in the occurrence of "high-temperature" superconductivity, and to draw conclusions on the interdependence of superconducting transition point, T_C, and phonon anomaly frequency, ω_E, electronic density of states, $n(E)$, (deduced from γ), material composition, vacancy concentration and, finally, the lattice dynamical parameters θ_0 and $\theta(T)$.

Specific heat data provide, in many cases, a crucial test of the overall feature of lattice dynamical models. However, the above-mentioned example illustrates that even interesting details on the phonon spectra may be detected at least at low temperatures. It should be mentioned that the anharmonicity of lattice vibrations and the surface lattice vibrations in small particles ($\phi < 1000$ Å) cause considerable excess heat capacity in addition to normal harmonic vibrations (as an example, see ref. 83).

2.3 Magnetic contributions

The behavior of magnetic materials at low temperatures is of widespread interest, since, by definition of thermodynamics, the specific heat $C_{H,M} = (dQ/dT_{H,M}) = T(\partial S/\partial T_{H,M})$ and $C_H/C_M = (\partial M/\partial H)T/(\partial M/\partial H)_s$; $\partial M/\partial H = \chi$ is directly correlated to the magnetization, M, and susceptibility, χ. A full discussion of these questions may be found in the many reviews on this subject[38].

Magnetic ordering from paramagnetic states to ferro (a), ferri (b), or antiferromagnetic (c) states occurs at sufficiently low temperatures if the exchange interaction overcomes the thermal randomization energy of the spins. The transition temperature, T_c, below which the spins become ordered, covers the range from a few

millikelvin up to 10^3 K. The behavior of such materials near the critical T_c value is typical for the general class of cooperative phenomena, and the behavior is reflected in specific heat anomalies.

This type of transition is exemplified by the specific heat anomaly of $NiCl_2 \cdot 6H_2O$, shown in Fig. 4 in a C_p vs. T representation[47]. Consider the tremendous rise of C_p and the resulting important energy content in the range between 2 and 10 K, compared with the normal electron and lattice contribution in the same temperature range.

A further type of anomaly of mainly magnetic origin, known as the Schottky anomaly, occurs if at least two (or generally more) low-lying energy levels separated by the ΔE_s are well separated from the remainder of the energy spectra. At $T \ll \Delta E_S/k$ (where k is the Boltzmann factor), the upper level will scarcely be populated, whereas at $T \ll \Delta E_S/k$, both levels are nearly equally occupied. The rapid change of internal energy in this two (or more) level system induces a huge additional specific heat contribution. The heat capacity due to Schottky anomalies rises exponentially at the low-temperature side, passes a maximum and then falls to zero with T^{-2} at sufficiently high temperatures. Typical examples of such anomalies are the paramagnetic salts[38] and the nuclear Schottky anomalies. Figure 5 shows a typical example, taken from ref. 48. It should be mentioned that some properties of such level-structured systems (number of energetic levels, energetic distance, degree of degeneracy) are deduced from the absolute specific heat values, from the resulting total entropy, from the position of the Schottky peak and from the specific temperature dependence. This, of course, assumes that the lattice and electronic contributions to the specific heat term are subtracted correctly. The problem of obtaining C_S, the specific heat due to the Schottky anomaly, is a considerable problem, which is solved by plotting C_pT^2 vs. T^5 at temperatures well above the peak, and $\ln C_p$ vs. T^{-1} far below the peak. Since $C_S \sim T^{-2}$, if $T \gg T_C$ the total specific heat has the form $C_p \simeq \alpha/\theta_o^3\, T^3 + ST^{-2}$. On the low-temperature side $C_S \sim e^{\Delta E/KT}$ and therefore $C_p \simeq \gamma T + e^{\Delta E/K}$.

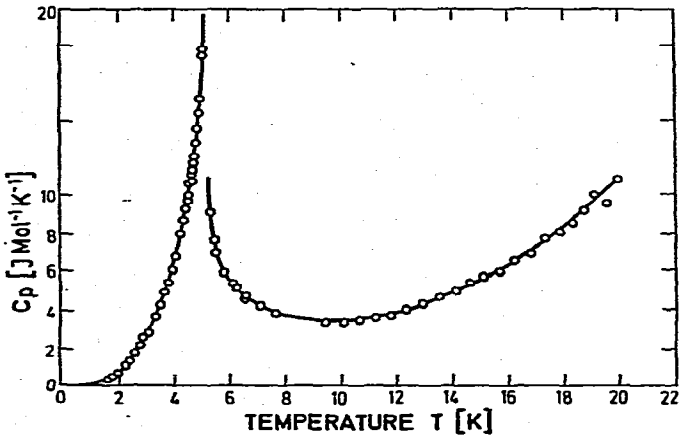

Fig. 4. (Taken from ref. 47.) Specific heat C_p of $NiCl_2 \cdot 6H_2O$ as a function of temperature T. The anomaly at 5.34 K is due to an antiferromagnetic transition.

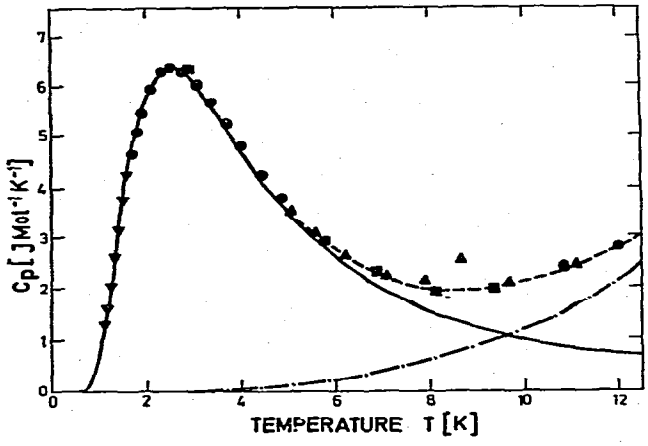

Fig. 5. (Taken from Ref. 48.) Specific heat C_p of α-$NiSQ_4 \cdot 6H_2O$ as function of temperature T. ▼, ●, ▲, Experimental points; ——, smoothed total specific heat C_p; –.–.–, lattice contribution to C_p; ———, contribution of Schottky anomaly to C_p.

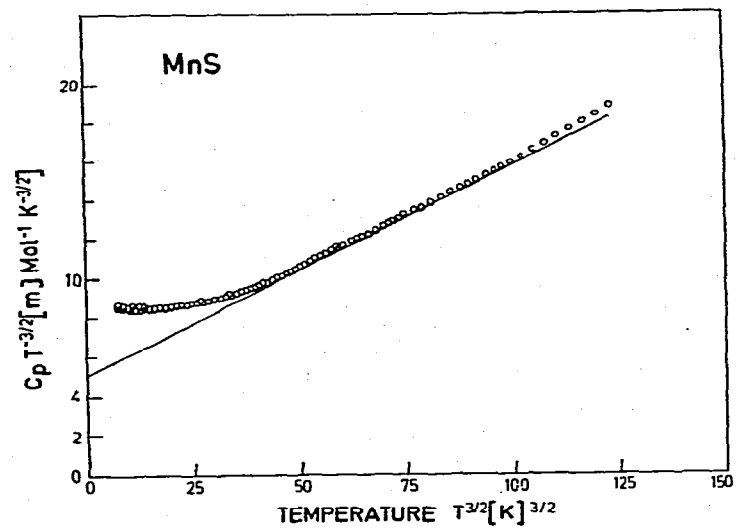

Fig. 6. Specific heat $C_pT^{-3/2}$ of MnS as function of $T^{3/2}$. ○○○, Experimental data; ——, representation of the formula

$$CT^{-3/2} = S(J) + (\alpha/\theta^3)\, T^{3/2}$$

From the linear representation the lattice term and magnetic exchange interaction are determined by the slope and the ordinate distance of the straight line, respectively. The deviation at low temperatures is caused by the "high-temperature" tail of a Schottky anomaly below 1 K.

The ideal ordered state in magnetic materials exists only in the absence of thermal agitation, otherwise the appearance of spin-waves is observed. The analogy between spin-waves and lattice vibrations is actually very deep. Analogous to phonons, the spin-waves quantize into magnons which play the same role in magnetic phenomena as phonons do in lattice dynamics. Magnons obey Bose–Einstein statistics and make contributions to the low-temperature specific heats which have the form $C_m^{\text{ferro}} = S(J)T^{3/2}$ or $C_m^{\text{antiferro}} = S'(J)T^3$.

A specific heat contribution in MnS induced by ferromagnetic spin-waves is illustrated in Fig. 6 (ref. 49). The appropriate plot is $CT^{-3/2}$ vs. $T^{3/2}$, thus representing in a linear form the lattice term C_1 and the magnon term C_m^{ferro}: $CT^{-3/2} = S(J) + (\alpha/\theta^3)T^{3/2}$. It should be mentioned that the simplified description of magnons, leading to the $T^{3/2}$ or T^3 dependence is valid only in a moderate temperature range. Often, deviations at low temperatures lead to an exponential T dependence whereas at higher temperatures, additional terms must be taken into account. Nevertheless, such a measurement immediately gives the quantum mechanical exchange constant J, included within the constant S above.

2.4 Cooperative phenomena, anomalies

There are various possibilities to classify abnormal variations of the specific heat. Several examples of unusual behavior can be ascribed to magnetic properties of solids, as illustrated above. A comprehensive discussion and many references may be found in the book by Gopal[38]. The term "anomaly" should be attributed only to unknown effects. In the sense of this definition, many anomalies reported earlier have later been revealed to originate from experimental shortcomings. Under conditions of a physical system, where the interaction among the constituents is so strong that the energy level of one partner depends on the energy states of its neighbors, or in other words, if the degree of occupation of a state influences the probability of occupancy of this state, cooperative phenomena may occur. The consequence is that such cooperative transitions of particles produce pronounced singularities denoted as "λ-anomalies" in the specific heat. Several examples are

(a) electronic transition, e.g. superconductivity, as shown in Fig. 7[50], magnetic dipole ordering, spontaneous electric polarisation (ferroelectricity);

(b) crystallographic transition, change from one lattice type to another;

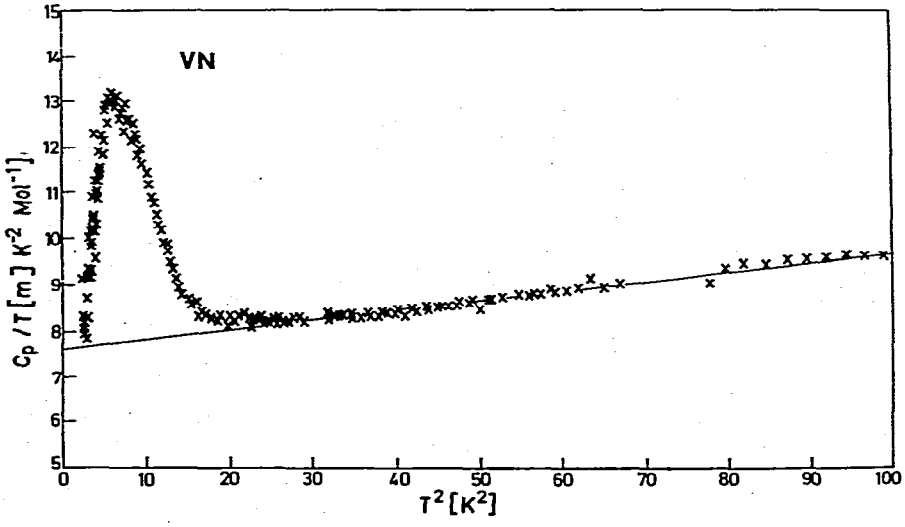

Fig. 7. Specific heat C_p/T vs. T^2 of VN. ×, Experimental points; ——, representation of $C_p = \gamma T + (\alpha/\theta_0{}^3)T^3$ with $\gamma = 4.7$ mJ/mole K^2 and $\theta_0 = 576$ K. The anomaly shows the transition to the superconducting state at $T_C = 3.4$ K.

(c) order–disorder transition as the classic example of β-brass, CuZn, in which at higher temperatures the lattice sites are randomly occupied by Cu and Zn;

(d) superfluidity of liquid helium-4 and helium-3;

(e) onset of molecular rotational vibrations, e.g. NH_4Cl and many organic materials, invoked by additional degrees of freedom at sufficiently high temperatures (see also Fig. 1 as an example).

In contrast to cooperative ordering, there is also a number of abnormal specific heat curves in physical systems where the various modes are independent, named "non-cooperative systems". The Schottky anomaly is the best example. Obviously miscellaneous "anomalies" still remain unclassified, such as contributions to the specific heat from: point defects in highly disordered materials like solidified rare gases or irradiated solid materials; dislocations in plastically deformed or quenched samples; Einstein terms from "quasi"-single modes; surface specific heat, observable in small particles ($\phi < 1000$ Å) exhibiting a T^2 lattice term at low temperatures[83].

The impressive variety of application of low-temperature "specific heat-effects" proves the fundamental and vital interest in performing calorimetric measurements over a wide range of temperatures, starting at a few milliKelvin up to the highest available temperatures. Before going into the experimental methods, the underlying problems and difficulties should be outlined.

3. BASIC PROBLEMS OF LOW-TEMPERATURE CALORIMETRY

The outstanding problem of low-temperature calorimetry is the tremendous reduction of thermal energy by a factor of 10^4 to 10^7 obtained on cooling any material from 300 to about 4 K. This drastic decrease in energy is shown convincingly in Table 1. The difficulties which arise from this energy reduction are the basic problems which still prevent "low-temperature calorimeters" being commercially available.

To perform precise measurements, four essential conditions have to be fulfilled and the related problems solved.

(1) Creation of the general cryogenic environment and sample cooling.

(2) Control of thermal exchange between sample and neighborhood, and in some case to isolate the sample from surroundings.

TABLE 1

SPECIFIC HEAT C_p FOR COPPER

T (K)	*C_p (J/mole K)*
1000	29.45
300	24.56
100	16.23
4	0.0063
1	0.00074
0.1	0.000069

(3) High-accuracy thermometry and high precision electronic circuitry for control of heat to be added to sample or shields.

(4) Computing and convenient data treatment and interpretation, especially in the case of non-adiabatic conditions, low thermal diffusivity within the sample.

The creation of low temperatures within a bath cryostat by use of liquid nitrogen at 77 K, liquid hydrogen at 21 K, or liquid helium-4 at 4.2 K or even liquid helium-3 at 3.2 K and down to 0.3 K, today represents a well-known technique used in most solid state physics laboratories without any special difficulty[51].

A schematic drawing of an adiabatic Nernst calorimeter immersed in liquid helium is shown in some detail in Fig. 8. This Nernst-type calorimeter is today still a

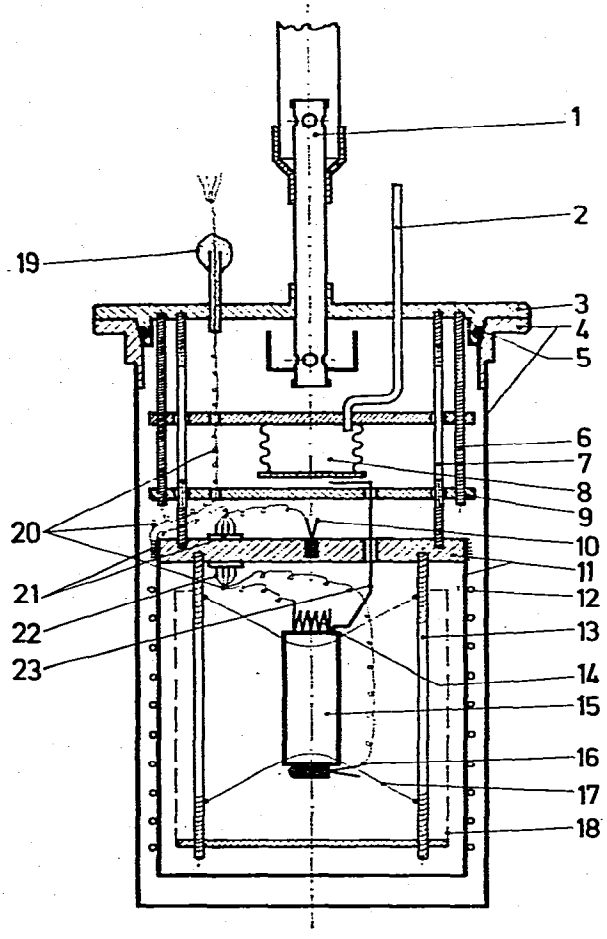

Fig. 8. Schematic view of an adiabatic calorimeter[52] for the temperature range 1.2–350 K, equipped with a mechanical-thermal switch and two regulated radiation shields. 1, Vacuum pumping tube with radiation shield; 2, pressurizing tube for bellow of mechanical-heat switch; 3, vacuum cell of calorimeter, top; 4, vacuum can; 5, indium seal; 6, support for heat switch; 7, support of radiation shields (stainless-steel rods); 8, bellows of mechanical-heat switch; 9, counterplate for bellows switch; 10, thermometer to control temperature of shield; 11, outer radiation shield; 12, heater of outer radiation shield; 13, support for sample holder; 14, sample heater; 15, sample; 16, sample thermometer; 17, cotton threads; 18, inner radiation shield; 19, electrical feed-through; 20, electrical wiring; 21, thermal anchoring of lead-wire; 22, electrical connectors; 23, gold wire as thermal contact between bellows and sample.

widely used technique and gives the highest available accuracy. The calorimeter shown should be regarded as representative of any other type of calorimeters, but details will be discussed in Sect. 4.2.2.

This calorimeter[52] consists essentially of a vacuum-tight cell (4) in which the sample (15) (a solid or a liquid within a container) is suspended thermally insulated. The heat capacity is measured by application of a known quantity of heat, Q, and simultaneous determination of the rise in temperature ΔT: $C_p = Q/\Delta T$.

The first problem arises from the need to cool the specimen to the temperature of liquid helium and subsequently to disconnect the sample thermally from the calorimeter assembly. Generally, helium exchange gas is introduced into the cell (4) providing convenient and effective cooling; but the He gas tends to be strongly adsorbed onto the sample surface, particularly in the case of porous or powdered samples. The use of exchange gas therefore requires properly designed pumping systems and, in most cases, long degassing times (several hours). It is preferable to avoid the application of exchange gas altogether and to apply mechanical–thermal switches.

Lowering the sample onto the base of the measuring cell for cooling and then lifting the sample with a simple windlass was successfully used by Keesom and Kok[53] and Westrum et al.[54]. Simple clamp-type heat switches have been described by Ramanathan and Srinivasan[55], Rayne[56] and Webb and Wilks[57]. Most of these devices require a delicate adjustment and sophisticated manipulation to avoid frictional heating during the opening of the switch. The bellows technique (see Fig. 8 and also Sect. 6) has been used successfully for years by the author[19, 52].

The control of the thermal exchange between sample and surrounding may be achieved in one of two different ways, by perfect adiabatic conditions or by non-adiabatic conditions, requiring an exact knowledge of heat exchange as a function of temperature. Both methods, which will be elucidated in the following sections, are based on a definitely known ambient. The calorimeters are therefore equipped with radiation shields. The isothermal or adiabatic (with respect to the specimen) shield techniques have been brought to a very high degree of refinement in recent years due to progress in thermometer sensitivity and electronic circuitry[7, 58, 59]. The use of extremely thin electrical measuring wires ($\phi < 0.07$ mm) for thermometer and heater and careful thermal anchoring of the electrical leads coming from room temperature into the cryostat to 4 K are required to avoid heat leaks. The problem of good thermal anchoring of wires of different cross-sectional area and various thermal and electrical conductivity has been thoroughly investigated[60]. High vacuum ($p < 10^{-6}$ torr) suppresses the residual gas conduction. Finally, the use of a small measuring current and the application of suitable high-resolution electronic devices will tend to minimize thermometer self-heating.

Table 2 gives an overview of the heat exchange between sample and surrounding shield, calculated for a typical calorimetric apparatus as shown in Fig. 8 and described in Sect.4.2.2.

To reach still lower temperatures, below 1 K, one has to use the helium-3

TABLE 2

HEAT EXCHANGE BETWEEN SAMPLE AND RADIATION SHIELD IN ERG/SEC, IF THE TEMPERATURE DIFFERENCE AMOUNTS TO ΔT

	1–4 K	*20 K*	*100 K*
Residual gas	$\pm 0.2\Delta T$	$\pm 0.2\Delta T$	$\pm 0.2\Delta T$
Thermal radiation	—	1	$85\Delta T$
Thermal conduction			
—Nylon lead suspension	$\pm 1.1\Delta T$	$6\Delta T$	$14\Delta T$
—Electrical	$\pm 0.3\Delta T$	$5.2\Delta T$	$12\Delta T$
Vibrational heating	0.5	0.5	0.5

isotope as a coolant, to make use of He 3/4 dilution refrigerators or an adiabatic demagnetization apparatus. By such means, temperatures of a few milliKelvin can be attained[61]; then the problems multiply. In order to suppress mechanical vibrations, attention has to be paid to anti-vibrating devices; vibrational energies must be less than a few tenths of an erg/min. The reader will find a thorough dicussion of the related problems in ref. 61.

There are many problems associated with thermometry. Commercially available calibrated semiconductor thermometers of germanium or gallium arsenide of high reproducibility and sensitivity ($\Delta T/T < 10^{-4}$) are available for the range 50 mK to 100 K. Platinum resistors are most practical and widely used above 30 K. Nevertheless, highest precision calorimetry even today requires recalibration and checking of these thermometers against the helium-3 or helium-4 vapor pressure scale as well as against the IPTS (International Platinum Temperature Scale) in the higher temperature range[7].

Detailed discussions of the thermometers, thermometry and related problems may be found in recent reviews on this subject[36, 37]; thermometry below 1 K has been reviewed by Hudson et al.[62] and discussed by Richardson[63] and Parker and Coruccini[64]. Attention should be drawn to the basic importance of establishing a precise temperature scale for calorimetric research; the precision needed is one of the highest in any solid state research, typically $\Delta T/T \sim 10^{-5}$ in absolute temperature.

The last step in the determination of specific heats is the analysis of the primary data. This requires

(a) fit of the observed data to smooth values;

(b) elimination of falsifying measurement points, e.g. during shield regulation;

(c) adjustment and correction for heat leaks. However, in practice heat exchange is very small since automatic shield regulation is sufficiently precise to minimize this correction;

(d) reduction of measured data to molar basis. This is done by subtraction of the "addenda" heat capacity — the heat capacity of sample holder, thermometer-heater unit or of the calorimetric vessel itself — and subsequent computation of the net specific heat of the sample in a convenient unit. The "addenda" heat capacity must be determined at least as accurately as the total heat capacity of the sample

(plus calorimeter) and therefore this tare heat capacity is measured in a separate run;

(e) reduction of data due to known systematic errors such as influence of actual room temperature on the normal resistances for thermometer current calibration, systematic errors of DVM's, etc.;

(f) elimination of systematic errors due to different heat exchange in different calorimeters. For a careful check, the same sample should be measured in different calorimeters in the same temperature range. The measurement of a copper standard sample[40] in the low-temperature range between 0.3 and 30 K presents a very precise test. Data has to be corrected for curvature in the region of T^3 law. Occasionally, when the ΔT increment during a heat-step is unusually large ($\Delta T/T > 3\%$), an appropriate non-linear interpolation must be made to determine the mean temperature[7];

(g) finally, extremely careful handling and checking of the temperature scale is a stringent requirement. The computer fit to an analytical mathematical law (e.g.

$$T = \sum_{i=0}^{n} a_i (\ln R)^i \qquad \text{(typically, } n \leqslant 10\text{)}$$

for a semiconductor resistor) should be made better than 1‰. It is easy to understand that the derivative of the difference in temperature between calibrated and fitted temperature values $d(T_{cal} - T_{fit}) = d(\delta T)$ must be smoothed, since $d(\delta T)$ directly influences the systematic error on C_p by errors of the temperature increment ΔT during the measurement.

An extended treatment of possible systematic errors and details of data treatment related to the calculation of thermodynamic functions is given in the paper of Westrum et al.[7].

4. ADIABATIC CALORIMETERS

4.1 Nernst calorimeter: pulse heating

The adiabatic calorimeter is still the most widely used technique and gives the highest accuracy. This "pulse heating" method is a direct transposition of the definition

$$C(T) = \lim_{\Delta T \to 0} \frac{Q}{\Delta T}$$

into a measurement: the energy Q apported and the temperature increment ΔT are determined at the sample. In principle the experimental problem is simple; it reduces to isolating the specimen from its surroundings and to measuring Q and ΔT as accurately as possible. The principle of the adiabatic technique is shown in Fig. 9. The equilibrium or steady state temperatures are determined before and after electrical heat input; a small drift rate is allowed to occur. Heat interactions between sample and calorimeter are computed from the observation of the temperature drifts at known times and the appropriate correction is made. A comprehensive review of several contemporary, high precision, adiabatic calorimetric cryostats suitable for the determination of heat capacities from about 4.2 to 350 K has been given by Westrum

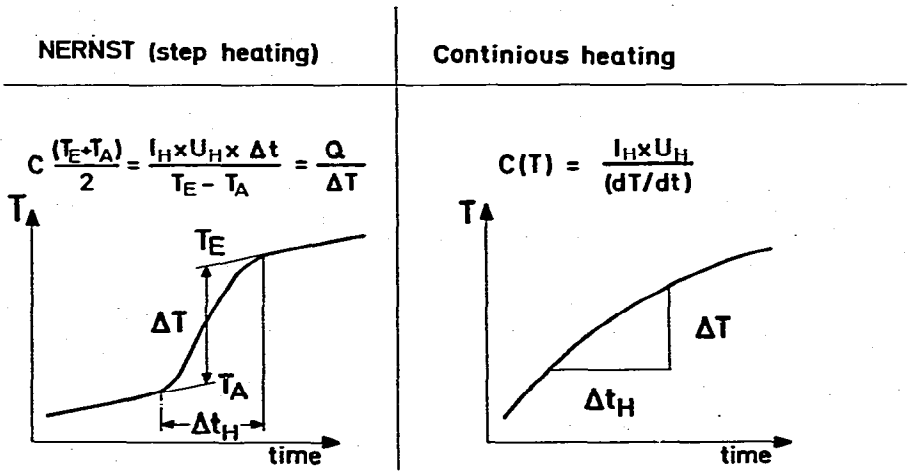

Fig. 9. Principles of adiabatic calorimetry. I_H, Heating current; U_H, voltage across heater resistance; T_E, final temperature (after heating); T_A, initial temperature (before heating); Δt_H, heating time; ΔT, temperature increment.

et al.[7]; further detailed descriptions are credited to several groups[65] and to work cited in refs. 11, 13, 15, 18, 19, 52.

Therefore, we focus our description on one representative Nernst calorimeter, for which the essential effort has been directed to complete automation. The high flexibility of the system is ascribed mainly to the high degree of automation, which enables the system to be used in a wide range of varying parameters as temperature 0.1 to 500 K, sample weight (0.5 to 500 g), thermal diffusivity (0.1 sec to several minutes within sample). At the same time this calorimeter illustrates the contempory technique and the different related problems to be overcome.

4.2 A fully automated adiabatic calorimeter

4.2.1 General. Several systems to automate specific heat experiments have been described in the literature. Considerable reduction in time was brought about by automatic data enregistration, carried out by Moody and Rhodes[8], Blythe et al.[9] and Kollie[10]. Martin and Snowdon[11] rigidly automated the entire experiment. Several real-time automatic systems able to record data and yield results during the experiments have been described recently by Pinel and Lebeau[12], Novotny and Meincke[13], Shin and Criss[14]. Nevertheless, the described installations require that the experiment is controlled manually and simple decisions on the experimental parameters must be made. Rapid variation of the specific heat at low temperatures or in the neighborhood of anomalies necessitates frequent adjustment of the experimental parameters as, for example, the heater current and the shield-control parameters. In this regard only an on-line computer technique achieves complete automatic and optimal operation of the calorimeter, since it is able to make decisions about the experimental control parameters on the basis of the results obtained. Such a computerized controlled calorimeter was described first by Martin et al.[15] and recently by Schwall et al.[16], Joseph et al.[17] and Moses et al.[18].

The experiment to be described is part of an integrated system which simultaneously controls four different types of solid state physics experiments[66]. The electronics is composed of standard CAMAC instrumentation. The adiabatic calorimeter is equipped with one or two computer-controlled adiabatic radiation shields. Continuous heating operation may be selected (see Sect. 4.3).

The computer-controlled experimental processing and data evaluation assembly may be applied to three different types of adiabatic calorimeters:

(i) a small calorimeter (o.d. 48 mm) with one regulated thermal shield for the range 1.5–90 K, designed to fit into a 2-in. superconducting solenoid, to perform heat capacity determination in the presence of high magnetic fields up to 10 Tesla;

(ii) a large calorimeter with two temperature-controlled adiabatic shields, used for measurements in the range 1.5–320 K;

(iii) a calorimetric set-up, adapted for a helium-3 cryostat to do measurements in the 0.3–10 K range.

4.2.2 Cryogenic calorimeter. The calorimeter of type (i) (and ii) is shown schematically in Fig. 8. The entire calorimeter is immersed in a liquid helium bath cryostat. The calorimeter is entirely constructed from copper; the vacuum can (4) (48 mm diameter, 250 mm in length) is sealed by indium wire (5). The sample (15) is generally sandwiched between a small copper plate on one side on which the thermometer (16) is attached, and a strain gauge of 600 Ω, the heater (14) on the other side. Calibrated germanium or platinum resistors are used as thermometers. The thermometers are tightly fitted with Apiezon N grease into the copper cylinder and are hard-soldered onto the copper plate (weight ca. 0.3 g). The "sandwich" (copper plate with thermometer, sample, heater) is fastened together by a very small amount of Apiezon N grease and Nylon threads*. This assembly is suspended from the isothermal shield (11/13) by cotton threads (17). The shield itself is held from the vacuum can flange by three thin-walled, stainless steel tubes (7) with Teflon rods at their ends. The heat capacity of the addenda, copper-plate with thermometer and strain gauge heater, is determined by separate runs.

All electrical leads (20) to the calorimeter pass through liquid helium and then onto a thermal anchoring stage (21) via a copper-tube-Stycast 2850 GT feedthrough (19)[67]. The thermal anchoring must be done carefully[60] and it consists of a copper disc (11) which serves simultaneously as the upper part of the radiation shield (11), support for the interchangeable electrical connectors (22) and location for the thermometer (10) which controls the shield-temperature. The 0.07 mm o.d. copper wires are wound several times around the plate within a groove (21) for thermal coupling to the corresponding shield-temperature.

The electrical wiring (20) to the sample thermometer and heater (14) is made by 0.05 or 0.07 mm diameter copper and constantan wires as current leads and potential connections, respectively; their length is about 35 cm. The thermometer leads are connected in 4 wire d.c. technique; whereas for the sample heater the asymmetrical 3

* Nylon wire contracts strongly if cooled down to 4.2 K.

wire method[68] of connecting the heater leads was adapted to eliminate errors due to Joule heating within the current leads.

For sample cooling, a mechanical heat switch (2/8) of the bellow type[52, 69] is used. Therefore the sample holder is elongated by a thin gold wire which is adjusted between both plates (8 and 9) of the bellow switch as shown schematically in Fig. 8.

The gold-plated thermal copper shields (11 and 18) are controlled as isothermal* shields in the low-temperature region, whereas above 80 K the inner radiation shield is operated as an adiabatic** shield. The temperature of the inner shield is computer-controlled by separated Ge or Pt thermometers (10). The outer shield is matched by a differential Au–0.02% Fe/Chromel-P thermocouple set between inner (18) and outer (11) shields, in conjunction with a commercial temperature controller.

4.2.3 Principles of data processing and operation. The center of the installation is a PDP 11/15 computer which handles and controls programs of the various experiments on a real-time basis. It also drives the standard peripherals which the user requires for data computation. The experimenter does his dialog with this computer by teletype (TTY). A second PDP 11/20 is used only for data evaluation. Both computers are coupled by an asynchronous interface, which gives both PDP 11 access to a coupling disc. Control programs are stored on this coupling disc and loaded into the core memory of the process computer (PDP 11/15) as needed[66]. Experimental data are stored on the same disc for further evaluation.

The experiment is connected to the process controller PDP 11/15 by a CAMAC interface in conjunction with a data highway and the CAMAC crate, containing the various individual plug-ins needed for the experiment. Only the "crate" is located at the experiment.

Figure 10 shows a schematic diagram of the complete measuring cycle during a heat step with the Nernst method. Each heating period is between two drift periods, where no heat is supplied to the sample. First the drift of sample temperature, T, under isothermal shield conditions, is determined by n successive measurements at constant time intervals t_i. At present, the drift curve may be determined from a minimum of 3 or a maximum of 20 temperature readings; the interval time can be selected between 2 and 1000 sec. Then, the sample temperature is raised with a heating current I_H during the time interval t_H; both values I_H and t_H, are precalculated by the computer in such a manner that a chosen relative temperature increase is achieved. ($\Delta T/T$ = constant, e.g. $\Delta T/T = 1\%$ in most cases). Next, the sample is allowed to thermally equilibrate for a selected time t_R, adequately adapted to the internal thermal relaxation of the sample. Thereafter, the temperature drift is measured as before. The increase in sample temperature, $\Delta T = T_F - T_I$, is obtained by a linear fit and extrapolation of the corresponding drift rates towards the midpoint of the heating time interval t_H.

---

* This means, the temperature of the radiation shield is held constant during the measuring procedure, $\Delta T = 0$.

** The temperature difference between sample and shield is regulated to be zero, $\Delta T = 0$; the shield follows the sample temperature variations immediately.

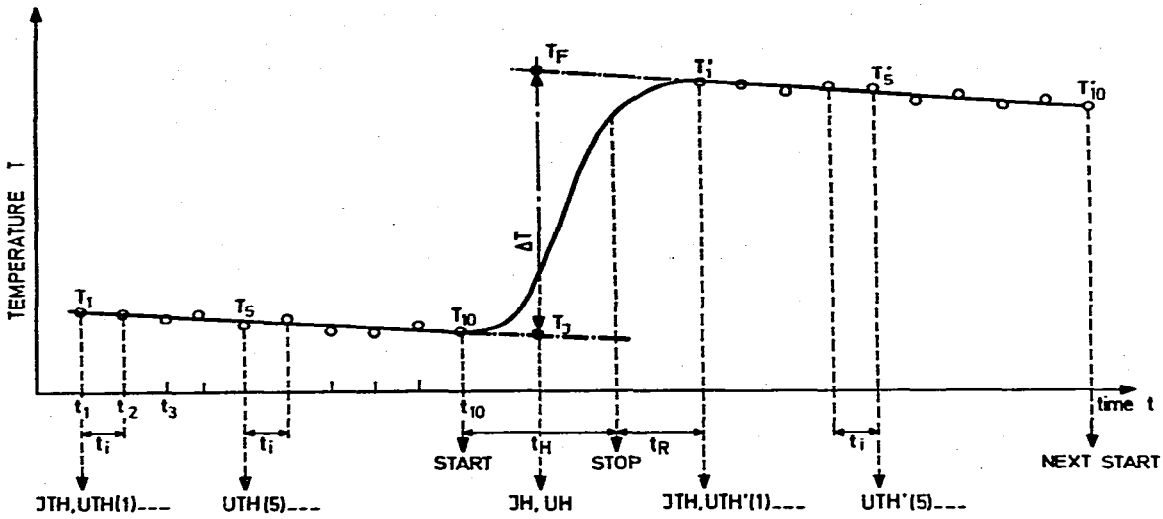

Fig. 10. Schematics of a complete measurement cycle for the automatic, adiabatic calorimeter. (Detailed explanation is found in the text.)

The calculated energy supplied to the sample during heating and the corresponding temperature rise yield the specific heat. This is evaluated during the next heating cycle. The heat capacity at the averaged temperature T_M, $C_p(T_M) = (I_H\ V_H\ t_H)/(T_F - T_I)$, where $T_M = (T_F + T_I)/2$ is calculated and the result is stored and printed on teletype. The high flexibility of this arrangement is due to the fact that suitable values for the following parameters can be chosen, depending on the special individual experimental situation:

(a) the number of temperature measurements, n, per cycle;
(b) the pause interval, t_i;
(c) the internal thermal relaxation time, t_R;
(d) the relative temperature increment, $\Delta T/T$;
(e) the temperature range to be measured; and
(f) the maximum allowed temperature drift of the sample, which depends on the properties of the sample and the regulating conditions of the isothermal or adiabatic shields.

Only for the first cycle do the heating time and heating current have to be preselected; for the following measuring cycles these values are calculated from the increased heat capacity. Optimized parameters are determined by test cycles and later inspection of the following runs.

4.2.4 Hardware. The experimental hardware applied to implement the discussed measuring cycle is shown in Fig. 11 as an electronic block diagram[19].

The experiment is branched by the data highway to the computer by a crate controller/transceiver unit. The circuits for the sample and shield thermometers as well as for the heaters are 4-wire d.c. circuits in which the effective thermo power is accounted for and in which the effective currents are measured by the voltage drop on standard resistors. An electronic 16-channel switch (multiplexer) connects the various

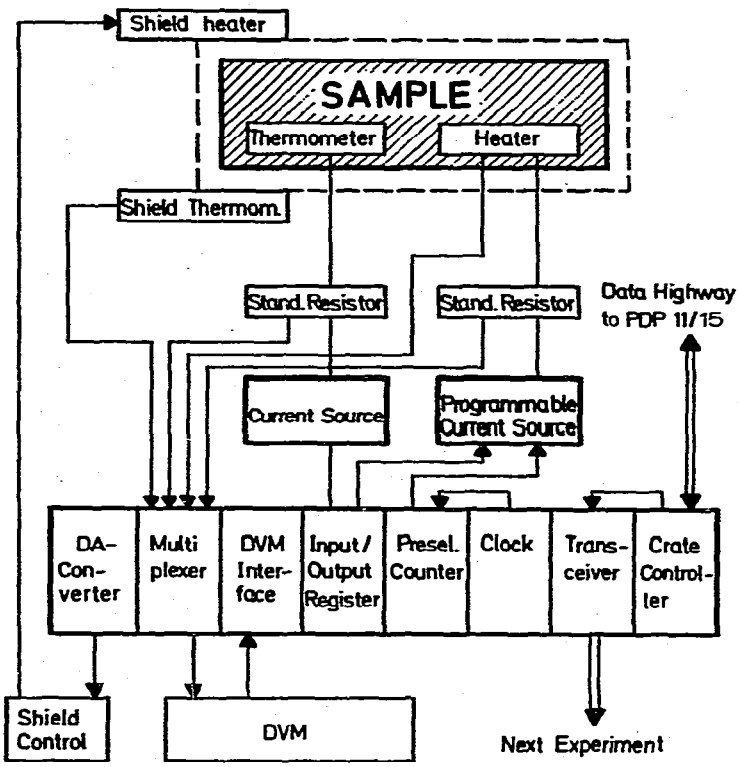

Fig. 11. Block diagram of hardware. Details are explained in the text.

voltages to be measured (heater voltage, heater current voltage, thermometer current and voltages, e.m.f.) to a programmable high resolution digital voltmeter.

The digital output of the DVM is read by the computer by the DVM interface and the transceiver/crate controller assembly. The thermometer currents are provided by two precision current sources ranging from 0.1 to 100 μA in 6 steps. They are set by the program via the input/output register. The heating circuit is built up in an analogous way. The heating current and heating time t_H are set by the input/output register and by the preselection counter, respectively, to the values calculated in the control program on the basis of the previously detected heat capacity. The preselection counter provides start/stop signals for the heater current source. This sample heating current source is based on CAMAC and is a highly stabilized wide range (10^{-9}–0.3 A), computer-controlled constant-current source[70].

The shield temperature, T_S, is regulated by a commercially available temperature controller. The temperature T_S is kept constant during the measuring cycles to better than 10 mK at $T < 20$ K and $\Delta T < 0.1$ K at $T > 30$ K, respectively.

If, in the case of isothermal shield control, the temperature drift of the sample becomes larger than a preselected value, the measurement is interrupted and the reference voltage coming from DA converter is increased to the sample temperature in order to raise the shield temperature, in order to reach "zero-drift" conditions.

The entire hardware is carefully isolated from the mains by separation transformers. The central grounding point is the computer to reduce the effects of electrical

interference; the guard shields are connected to the cryostat calorimeter assembly.

4.2.5 Software. The user identifies himself with the system by LOGIN CALMET and is then prompted for a service request by the string "MODE": the following software modules may then be selected:

PAR: Introduce the coefficients a_i for the thermometer R vs. T (resistance vs. temperature) relation

$$\left(\ln T = \sum_{i=0}^{n} a_i R^i\right)$$

TEST: Test measurements of voltages, resistances, temperatures on the different channels of the multiplexer.

MAN: Semiautomatic specific heat measurement.

AUTO: Completely automated specific heat measurement.

SAVE: Save measured data of AUTO and MAN made from current file CURRFI onto file CURSAV together with a dedicated text.

CLR: Clear of files CURSAV or CURRFI.

DETAIL: Print-out on TTY the information text of file CURSAV.

PRINT: Transfer data from CURSAV or CURRFI (on PDP 11/15) on the system's coupling disc onto one of three specified files (on the PDP 11/20) for further computation of the data set.

MTAPE: Selection of data-recording processes, for instance plots C_p vs. T, C_p/T vs. T^2, elimination of wrong data (e.g. taken during shield regulation), save of original data on tape or transfer of values to a large computer for evaluation of thermodynamic data: entropy, enthalpy, free energy, electronic specific heat, Debye temperature calculation, data listing and application of special FORTRAN programs.

STATUS: Request if Mode PRINT or MTAPE has been performed.

LOGOUT: Termination of the user's experiment.

In case of an emergency shut-down the contents of the status register and the current file data are saved.

In the following, only the AUTO mode will be explained in more detail. Figure 12 gives the dialog between operator–computer and the output results; this dialog is done via a teletype.

To start an experiment, the set of parameters for the calibration data of the thermometers has first to be keyed in the PAR mode. Then selection of mode TEST gives the actual resistance and temperature values to the operator. After selection of mode AUTO the experimenter is requested (see Fig. 12) to read-in: the experiment number, #; the correct thermometer parameter sets NR SHIELD and NR SAMPLE corresponding to the temperature range to be covered; the mathematical function to represent the addenda heat capacities CB (previously measured in a separate run); the mole number of sample MOL; and suitable values for the following parameters depending on the experimental situation (see also Fig. 12): number of temperature measurements per cycle STEPS, interval time t_p, INT, thermal equilibrium time τ,

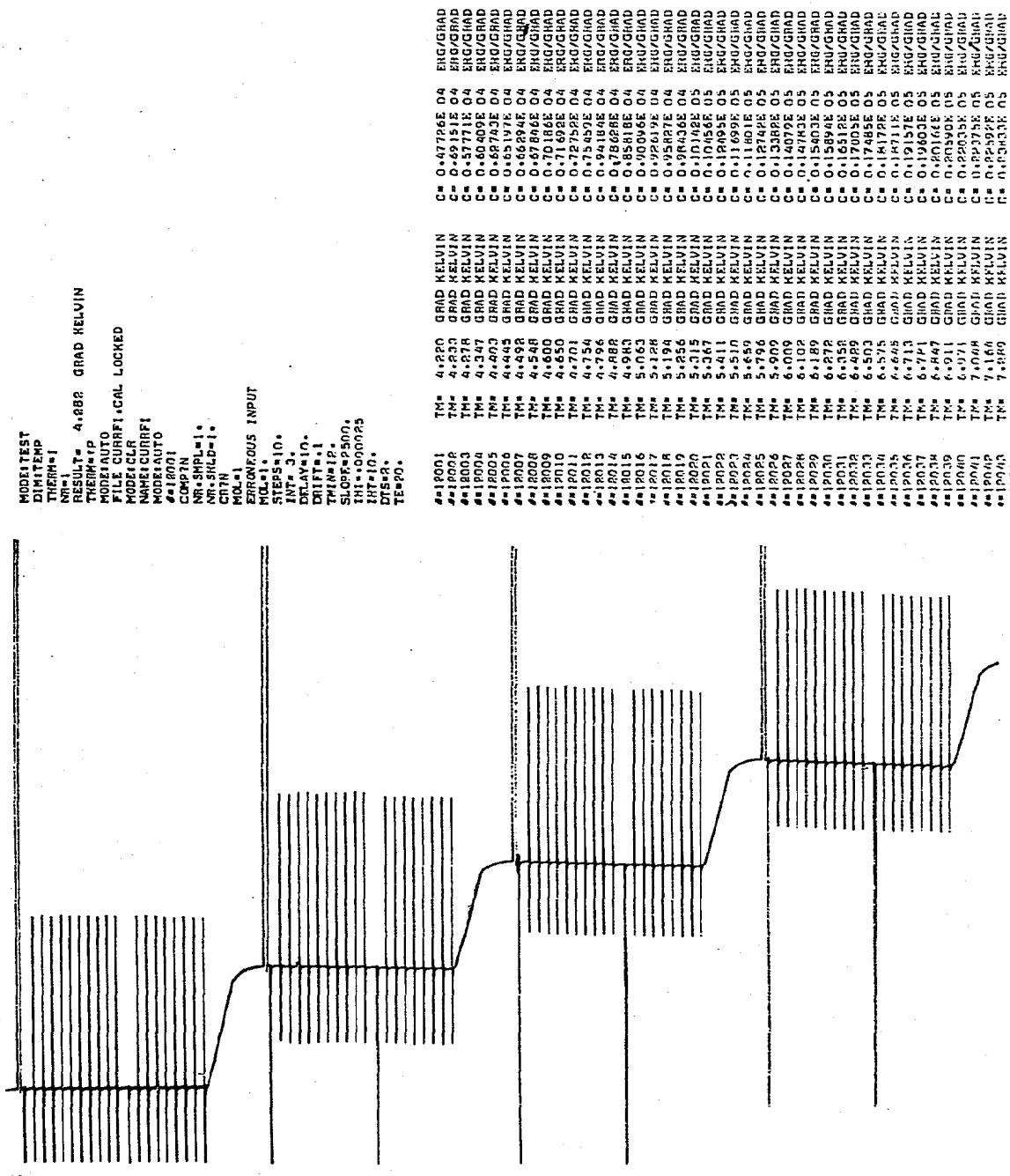

Fig. 12. Photograph of teletype print-out, of parameter input and data output dialog between experimenter and computer. Details are explained in the text.

DELAY, maximum temperature drift admitted for the sample DRIFT, the fundamental parameter DTS, the relative temperature increase per heating cycle and temperature range (maximum temperature) TE. For the first measuring cycle the heating time IHT and heating current IHI have to be adequately preselected. If the sample holder heat capacity is known it may be stored in the form of a polynomial and directly subtracted from the total measured heat capacity.

After definition of all these parameters, the measurement is started and the full cycle described in Sect. 4.2.2 is completed. The completion of such a cycle requires at least 20 sec at the lowest temperatures and up to 30 min at 300 K. Then the results for T_M and C_p are printed on teletype (Fig. 12) and all acquired data are stored on file CURRFI of the coupling disc for further inspection and evaluation.

4.2.6 Performance. The calorimeter described above has been applied to the study of a large number of samples between 0.4 and 350 K[41, 44, 45, 46, 50]; the absolute accuracy was tested by measurement of a standard copper sample[19]. A maximum error of 0.5% or less can be achieved.

The automated calorimeter has been proved to have a very large flexibility in selecting the appropriate system-control parameters which are optimized to the experimental boundary conditions given by a certain sample: temperature range, from 0.3 K to room temperature, low or high thermal diffusivity, large or small (100 mg) mass of the sample to be measured and high accuracy in the vicinity of specific heat anomalies.

The Nernst method actually yields the highest attainable accuracy, in some cases 0.1% or better. The advantage of this method is that the heat is applied intermittently in pulses, the total heat input, even under non-adiabatic conditions, is correlated with the temperature difference between the initial and final states of quasi-equilibrium. Heat leaks through sample suspension threads, residual gas and radiation can be kept low or sensibly constant and any residual heat exchange is corrected for, so that it does not affect the measurements.

In the Nernst method, a correction for any extraneous heat input is found directly for each heat pulse. A second advantage arises from the direct indication of the internal thermal relaxation time of the sample, if thermometer and heater are separated on the sample. There is inevitably some thermal resistance within the system, heater–sample–thermometer. The actual recorded temperature may differ considerably from the sample temperature during a heating period; the heater may be overheated. The time needed to re-establish equilibrium is shown during recording of a heat pulse step by the "delay" (Fig. 12). It is evident that the corrections can easily be made by extrapolation of the drift lines, provided an appropriate constant drift has been attained before starting the next point. Nevertheless, the method is tedious and is essentially restricted to point-by-point measurement, if the measurement is not automated, as in our case.

4.3 Continuous heating method

In the case of steady state heating[71, 72], in which heat is added continuously to the specimen at constant rate $P = I_H \times U_H$, only the resulting temperature increase is recorded. The heat capacity is given by the instantaneous derivative of the temperature T with respect to time t: dT/dt. The principle of the "continuous heating" method has been shown in Fig. 9 (right-hand side). Ideally, this technique requires an immediate distribution of heat within the addenda–specimen system and in the sample itself. To fulfil this requirement, the method is applied preferentially to small samples

of high thermal conductivity. Otherwise, precautions have to be taken (i.e. copper fans within the sample) to provide rapid internal thermal equilibration; the heat inputs should be chosen small enough to guarantee a uniform distribution of the temperature. To avoid misleading, calorimetric data the following condition should hold[21]

$$\frac{dT}{dt} \ll \frac{(T_F - T_I)}{\tau_i}$$

The requirement of a rather short internal relaxation time τ_i restricts the general application of this method considerably; only materials having a high thermal diffusivity can be investigated without any problems. This is true, for instance, for metals below 100 K. However, it should be noted that a state of dynamic thermal equilibrium is present even in samples of low thermal conductance and that the relative variation of $C_p(T)$ can be resolved to better than 1 % in any case. The precision of the measured absolute C_p data suffers from the fact that no direct control of extraneous heat interaction can be carried out as with the discontinuous heating (Sect. 4.2). This advantage may partially be overcome by direct evaluation of the sample–surroundings heat exchange by the following operational procedures: either to stop the heat input and to observe the remaining temperature drift caused by the heat leak, or by repeating the heat capacity measurements with different electrical heat inputs. Investigations of the internal relaxation time τ_i may also be performed in the same way.

The continuous warming method provides a continuous read-out of $C_p(T)$ data and has the additional advantage of speed and simplicity which leads to the possibility of a considerable degree of automation. The large amount of data taken continuously makes it possible to raise the accuracy by statistical methods of analysis. The data scattering and reproducibility may be 0.1 % or better[73]. (The heat leak is less than 0.1 erg/sec; the temperature accuracy exceeds 1 μK at 4.2 K.) The method is especially suitable for the investigation of sharp structures in the specific heat as transition peaks or anomalies* and to detect small variations of $C_p(T)$ in limited temperature ranges.

It must be noted that the method reaches the high absolute accuracy of the Nernst method only in a few favorable cases. In general, the absolute accuracy is less than in the discontinuous method, typically 1–2 % and the user has to pay careful attention to study the problem of internal heat equilibrium.

A detailed inspection of the described method has been given by Cochran et al.[71]; many experimenters have used the method successfully[12, 72, 73], especially in connection with automatic data acquisition[10, 12, 71]. Naito et al.[74] described a wide range of continuous warming calorimeters for temperatures from 300 to 1.000 °C, which should also be applicable below 300 K, down to 100 K at least.

* When measuring peaks in $C_p(T)$, the τ_I effect can again distort the result since the steep increase of C_p causes a corresponding rise of τ_I.

4.4 Adiabatic differential calorimetry

4.4.1 Dynamic differential calorimetry. The apparatus for determination of $C_p(T)$ from 2 to 300 K described by Lagnier et al.[75] uses two cells thermally isolated from each other and the surroundings. One cell contains the sample to be measured, the other being equal in mass of addenda is empty or encloses a reference sample. Both cells are surrounded by two screens. A schematic drawing is given in Fig. 13(I). The temperatures of the radiation shield (SC) are raised at a constant rate. The difference in heating power required for each cell (S_1) and (S_2) to follow the shield temperature is proportional to the thermal capacity of the samples and the rate of rise in screen temperature. The power difference between heaters (H_1) and (H_2) is directly analysed by a computer. The system proved very useful in the study of low-temperature anomalies and in the investigation of irradiation-damage effects, where the background specific heat of the unaltered material (reference sample) is automatically subtracted. This approach combines the advantages of the continuous warming method with the high absolute accuracy of the discontinuous method. Only 1% error in absolute calorimetric results has been detected with respect to standard samples.

4.4.2 Differential scanning calorimetry. Quasi-adiabatic differential scanning calorimeters (DSC) are commercially available[76] for temperatures above 120 K. The apparatus needs special and careful temperature calibration in the range below room temperature. There is obviously no serious restriction to the use of these devices at still lower temperatures, except the requirement for more adequate design of the cryogenic parts. The calorimetric resolution for specific heat measurements does not exceed 2% below 200 K.

4.4.3 Other methods. Recently, Jones et al.[77] used a differential technique to measure the ratio of specific heats of two samples with an accuracy of 0.25% or better

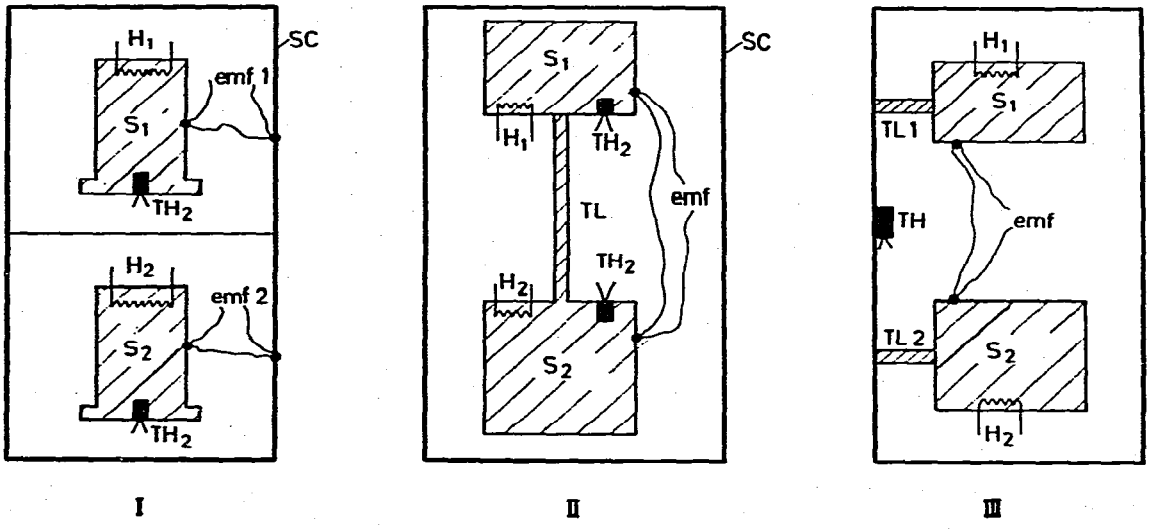

Fig. 13. Schematics of differential measuring techniques. I, Differential, adiabatic calorimetry[75]; II, differential, non-adiabatic calorimetry[76–78]; III, differential, relaxation-time calorimetry[79]. S_1, Sample 1; S_2, sample 2 (reference); H_1, H_2, heaters; TH_1, TH_2, thermometers; e.m.f., thermocouples; TL, thermal link; SC, screen for thermal radiation.

in the range 1.5–400 K; the absolute accuracy was 0.5%. The unique feature of the system, which is schematically shown in Fig. 13(II), is a heat leak (made from stainless steel) placed between the sample to be measured and the reference sample in order to maintain the unknown specimen in a near-equilibrium state.

Provided that the intrasample relaxation times τ_i are much shorter than the equilibrium time τ_e between both samples (ranging from 1 sec at 4.2 K to 20 sec at 400 K), heat pulses Q_1 and Q_2 applied to the heaters (H_1) and (H_2) on the samples, produce temperature increases of ΔT_1 and ΔT_2. A thermocouple (e.m.f.) detects the temperature difference $\delta T = \Delta T_1 - \Delta T_2$ between both. Therefore, the ratio of the heat capacity of samples (S_1) and (S_2) may be written as

$$\frac{C_p(1)}{C_p(2)} = \frac{(\Delta Q_1/\Delta T_1)}{(\Delta Q_2/\Delta T_2)} \simeq \frac{\Delta Q_1}{\Delta Q2}\left(1 + \frac{\Delta T}{\Delta \Gamma}\right) \text{ for } \Delta T_1 \simeq \Delta T_2$$

The advantage of the system is obvious: the ratio of C_p is much less temperature-dependent than the specific heat and therefore the relative sensitivity is considerably increased[77].

To complete the enumeration of methods, it should be mentioned that Marx[78] described a further differential technique, relying also on two samples connected by a "weak link". Alternating application of heat pulses into sample (S_1) or (S_2) (see Fig. 13 (II)) causes different heat flows in opposite directions across the weak link TL. The temperature difference, created along the weak link TL is detected by several thermocouples distributed along this thermal leak TL. The detected temperature variations are proportional to the heat flow and inversely proportional to the heat capacity of (S_1) and (S_2).

The basic advantage of the differential techniques is firstly the high relative accuracy — absolute calorimetry must be based directly on reference standards — and secondly the elimination of systematic errors, due mainly to uncontrolled heat exchange with surrounding, residual gas and temperature radiation. Both samples are subject to the same experimental condition. The limiting factor and source of uncertainty are primarily the internal equilibrium times τ_i within the samples, depending on the thermal properties of the samples themselves; the dependence of τ_i on the absolute temperature; and the influence of the unknown heat exchange, if the surrounding conditions are not kept identical.

Nevertheless, in the last decade these methods opened a large field of promising development and will be used more and more, since the differential techniques combine high absolute and relative accuracy with rapid and simple measuring techniques.

5. NON-ADIABATIC METHODS

Non-adiabatic calorimetric methods have emerged from the need to do specific heat measurements under the condition of poor thermal isolation of the sample from

the surroundings and the need of a very simple heat switch to initially cool the sample to the lowest obtainable temperature.

The usual adiabatic methods, discussed above, are not suited for measuring small heat capacities as in the case of either very low temperatures ($T < 1$ K) or very small samples (masses $m < 100$ mg). The ratio of applied heat per unit time by the heat conductance along the electrical measuring lines is far too large to be tolerably compared to the small total heat capacity of the samples. To investigate pressurized samples also adiabatic conditions cannot be achieved. Furthermore, a reliable heat switch must have frictional heating as it opens and the motion to activate the switch must be transferred from room temperature to very low temperatures. Frictional heat, vibration and bulky mechanical construction are rather difficult to add onto ^{3}He cryostats or $^{3/4}$He dilution refrigerators. Superconducting switches may be used below 1 K, but do not provide adequate thermal isolation of small samples above 1 K.

To overcome such difficulties, two new methods have been developed, the a.c. method of Sullivan and Seidel[20] and the relaxation-time calorimetry of Bachmann et al.[21]. Both methods have been applied with great success in the past[80–83], not only in the originally described arrangement used in the liquid helium range, but also with slight modifications at higher temperatures. Extensions of the method to temperatures below 1 K have been successful[82].

5.1 A.c. method and relaxation-time method

The principle of both methods is shown in Fig. 14. The basic idea is depicted in the middle of the diagram. The steady state a.c. method and the thermal relaxation method utilize a permanent thermal link between sample C, T (having heat capacity c and temperature T) and the low-temperature bath T_0 in order to eliminate any type of heat switch and to cool small samples in the presence of vibrational heating.

In the a.c. method (left-hand side of Fig. 14), heat $P(\omega)$ is applied at a frequency ω to the sample. The component of the resulting temperature amplitude is given by

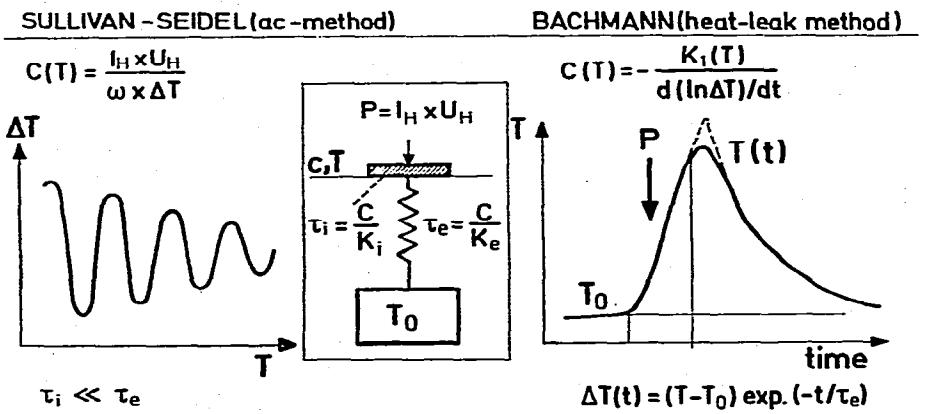

Fig. 14. Principles of non-adiabatic calorimetry. A schematic arrangement for both techniques (a.c. and relaxation-time method) is shown in the middle of the picture. C, T, Sample; T_0, constant temperature block; —WW—, thermal link; P, heating power; τ_i, τ_e, internal (intra-sample) and external (sample-block) relaxation times.

TABLE 3

COMPARISON OF METHODS TO MEASURE SMALL-SAMPLE HEAT CAPACITIES

Method	*Definition*	*Time constant*	*Typical sample size (g)*	*Condition for 1% accuracy*
Nernst-method	$C_p = Q/\Delta T$	$\tau_e \gg$ minutes	>0.2	$10\,\tau_e > t_H > 5\,\tau_i$
Continuous warming	$C_p = P(T)(dT/dt)^{-1}$	$\tau_e > 10\,\tau_i$	>0.1	$(T - T_0)/\tau_i \gg dT/dt$
Sullivan–Seidel (AC-method)	$C_p = 1/\Delta T_{ac}$	τ_e short	0.001–0.1	$(\omega\tau_e/10) > 1 > \omega\tau_i$
Bachmann et al. (relaxation-time method)	$C_p = k_e\tau_e$	$\tau_e > 5\,\tau_i$	0.01–1	$\tau_e \gg \tau_i$

$\Delta T = P_{ac}\,(\omega C)^{-1}$ (P_{ac} equals the ω component of the applied heat: $P = P_0 \sin\omega t$). The heat capacity results in a quite complicated formula, but which can be written in first-order approximation: $\Delta C(T) = P(\omega)\,(\omega\Delta T)^{-1}$*. This method is contrary to the adiabatic calorimetry: there is no more need to wait for equilibrium of the external relaxation time τ_e (see Table 3), provided the internal relaxation time $\tau_i = c/k_i$ (k_i internal thermal conductivity) is short enough. All parts of the sample assembly, including the heater and thermometer, must obtain thermal equilibrium in a time τ_i short compared with the inverse of the frequency ω of the heater current.

In addition, the method gives a continuous read-out of the heat capacity. Difficulties may arise if the internal τ_i is low, since there will be a temperature gradient within the sample itself. Therefore, the detected ΔT signal would not reflect exactly the heat capacity[21]. To achieve a 1% accuracy the following condition must hold

$$\omega\tau_e/10 > 1 > 10\omega\tau_i$$

Sullivan and Seidel[20] and Manuel et al.[80] have investigated in detail the various combinations of the parameters τ_e, τ_i, C, k_i, k_e, T_0 and ω. The reader is referred to the original papers, since a discussion of the many possibilities exceeds the scope of this contribution. Several interesting modifications have been described in literature, e.g. Handler et al.[81] obtained data on temperature intervals of less than 0.01 K by heating a foil sample periodically by chopped light (26 Hz).

The thermal relaxation-time method[21] is shown diagrammatically on the right-hand side of Fig. 14. The sample is heated by power P during a certain time. If this power is cut off, either after steady state has been reached or during temperature increase, the following decay of $T(t)$ to T_0 occurs exponentially with a time constant C/k_e

$$T(t) = T_0 + T\exp(-t/\tau_e) \text{ or } C = \frac{k_e(T)}{d(\ln \Delta T)/dT}$$

* The frequency, ω, is of the order of several Hertz.

Both methods obviously require an appropriate adjustment of the thermal link. This is done by suitable choice of the material for the link, and its geometry, length and diameter. Optimization is achieved only for a rather limited temperature range (0.4–1 K; 1–4 K) typically varying by a factor of 4–6.

A principal advantage of the relaxation-time method compared with a.c. measurement is the possibility of measuring and controlling τ_e directly and therefore of measuring absolute calorimetric data, whereas the a.c. technique is more advantageous for detecting extremely small relative variations in C_p, e.g. by the application of an electrical or magnetic field or to studying effects which occur extremely close to critical temperatures. The a.c. measurement is a steady-state observation so that it may be averaged over long times for improving the signal-to-noise ratio.

Samples as small as 1 mg having heat capacities of less than 0.05 μJ K^{-1} have been measured using both of the outlined methods. The reproducibility of both types of measurement is better than 0.5%, the accuracy lies in the vicinity of 1%, if careful calibrations, study of the thermal conditions (τ_i, τ_e) and a rigorous test (measurement of Cu standard sample) are performed. The main difficulties in doing this type of calorimetry are the attachment of thermometer and heater to the sample and the suitable choice of the heat conductance of the thermal link.

The sample support very often consists of a thin (typically 100 μm) piece of sapphire or silicon, on which the heater, i.e. a Ni–Cr resistor of several hundred ohms, is evaporated. Thermometry may be performed either by doping of the silicon chip directly, by very small semiconductor resistors, exposed Ge elements, or by carbon resistors, evaporated or painted (Aquadag) onto the support. One serious complication is how to minimize the heat capacity of these small thermometers. Proposals have been made by several scientists[84]. In addition, these home-made thermometers must be calibrated in situ against other thermometers using an exchange gas. Generally, they are not repeatable after cycling to room temperature so that they must be recalibrated for each run. Currently, the components are held together by some bonding grease (Apiezon N).

A typical arrangement used by the author is shown in Fig. 15[44, 79]. Gold,

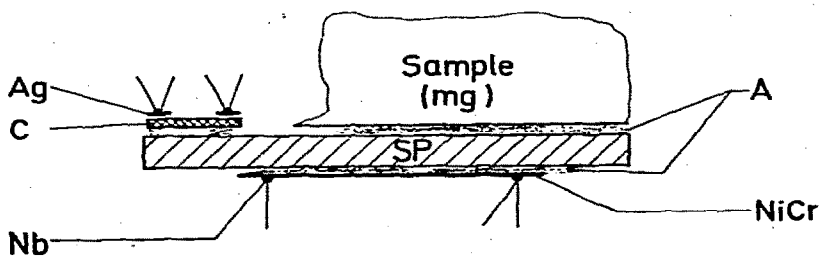

Fig. 15. Sample-holder assembly for non-adiabatic calorimetry with very small amounts of sample material (several mg and $T < 1$ K). SP, Sapphire plate as sample holder; 50 μm thickness, 10 mm diameter; A, thin layer of less than 0.1 mg Apiezon; Nb, electrical wiring for heater and thermometer, niobium: 0.03 mm diameter, which serves also as thermal link; C, sliced carbon thermometer, 2 × 2 × 0.2 mm; NiCr, evaporated Ni–Cr heater; 500 Ω; Ag, silver-paint contacts to heater NiCr and thermometer (C). The entire system is deposited on a wire-grid network of cotton wires in vacuum and surrounded by a radiation shield at temperature T_0.

platinum or copper wires have been used as thermal links (Cu: $\phi = 0.075$ mm; length = 25 cm; $k = 5 \times 10^{-4}$ W/K at 4.2 K and 10^{-6} W/K at 0.3 K). The sample assembly is surrounded and connected to a constant temperature reference block at T_0, where also the electrical connections (niobium wires, $\phi = 0.03$ mm) are thermalized by metal-coated sapphire heat sinks.

The advantage of using grease is that it may stay permanently on the sample holder and that it has proven to give good thermal contact (about < 0.1 mg). In addition, Apiezon grease minimizes the heat capacity, since the other low-temperature bonding agents — as GE-7031 varnish — have a heat capacity per gram/unit which is 5–10 times larger than that of copper.

Two serious difficulties arise in doing these experiments.

(a) The deposition of small amounts of cooling exchange gas on the sample surface can lead to large systematic errors. Therefore, the contamination of the sample surface should be avoided by pumping to high vacuum at room temperature followed by cooling by thermal conduction only; sometimes, the cooling time may exceed two days.

(b) The lowest attainable temperature is limited by spurious electrical and vibrational heat inputs into the sample. Anti-vibrating devices, which are normally used in very low-temperature research[51, 61] can reduce the energy input to less than 0.5 erg/min by putting the cryogenic part upon a massive concrete block, supported by appropriately selected springs (the system should have a natural frequency of about 1 Hz); connecting every vacuum and gas tube between the cryostat and the outside only by soft bellows which should be fastened on one side rigidly to the floor, or passed through sand boxes before reaching the bellows; careful shielding and grounding of all transmission lines of the cryostat and the electrical circuits against all disturbances, as radio frequency waves from TV stations, noise from electrical equipment in the vicinity. A particular nuisance is that carbon thermometers are especially susceptible to absorbing energy from radio frequency-fields. Usual remedies are to place mica capacitors or lossy ferrite beads in the electrical lines inside and on the top of the cryostat.

5.2 Differential relaxation time calorimetry

The principle of this technique is shown schematically in Fig. 13(III). Two nearly identical sample holder assemblies (S_1) and (S_2) as described in detail in Fig. 15 are employed in analogy to the simple relaxation-time method[21]. One sample support (S_1) serves to hold the unknown sample. The reference sample (e.g. sapphire or a copper standard) is placed onto the second support. This calorimetric measurement is a combination of a differential and relaxation calorimetry[79].

Simultaneous heat pulses (P_1) and (P_2) are applied to both support sample systems in such a manner that the resulting temperature increases (see Fig. 14, right-hand side) $\Delta T = (T - T_0)$ are equal. During the following relaxation, both $T(t)$ signals (from samples 1 and 2) are applied to opposite branches of a bridge: thus the compensation creates a signal deviating from zero by: $\delta(\Delta T) = \exp[-t\ (1/\tau_{e2} -$

$1/\tau_{e1})]$. In the first approximation, provided $\Delta T = T - T_0$ is equal at both samples, $\tau_1 \simeq \tau_e$, and $k_{e1} \simeq k_{e2}$ the ratio of heat capacities is proportional to the inverse ratio of the applied heats: $(C_1/C_2) = (Q_2/Q_1)$.

5.3 Combined measurement of thermal conductivity and specific heat

In addition to C_p, thermal conductivity λ, is among the most fundamental experimental investigations made on solids at low temperatures. Conventional d.c. methods meet with difficulties when applied at low temperatures. Thermal conductivity measurements involve similar problems. There exists a large field of techniques to determine simultaneously C_p and λ, also at high temperatures. Common to these methods is that one end of the sample, which has the form of a rod and is surrounded by vacuum, is kept in contact with a low-temperature reservoir while a heater is attached to the other isolated end of the rod. The methods developed until now should be mentioned only in principle.

Zavaritsky[85] developed a technique related to the a.c. method. The attenuation and the phase shift of a temperature wave is observed as it propagates through a solid rod. The rather elegant method appears to be extremely difficult. The main difficulty is to separate properly the unwanted temperature phase shift of the thermometer from the shift induced by the sample.

A pulse technique described by Bertram et al.[86] avoids this difficulty. In this method, a δ function of heat is generated in the heater and then the diffusion of this heat pulse throughout the sample rod is studied by different thermometers at various distances x from the origin

$$\delta T(x, t) = \frac{Q\, l^{-x^2/4Dt}}{(4\pi Dt)^{1/2} AC}$$

A simple calculation gives the heat capacity

$$C = \frac{Q}{(2\pi e)^{1/2} l A \delta T_{max}}$$

and the thermal diffusivity

$$D = l^2/2t_{max}$$

with, l, distance between thermometers; A, rod cross-section; T_{max}, maximum temperature signal at point l; t_{max}. time at which T_{max} occurs.

Since the diffusivity is given by $D = \lambda/C$, the pulse height and arrival time give values of C_p and λ. This technique is particularly well suited for measurement on specimens with small masses. Recently, this method has been further developed[87] with the help of a rigorous and convenient method of analysis derived by Gershenson and Alterovitz[88]. The authors were able to measure C_p and λ on thin films (1 × 3 cm, 75 μm thickness) of granular aluminium down to 1 K with a resolution of 0.2 μJ/sec K and $C_p = 0.01$ μJ/K.

A slightly modified method described by Gobrecht et al.[89] analyses also the propagation of the heat pulse — the time dependence and local dependence of the induced temperature increment $T(x, t)$ — within the sample. The method is applied in the temperature range 77–500 K and heating is performed by light flashes.

The transient hot-wire technique was recently extended to determine simultaneously C_p and λ[90]. The essence of this method consists of heating a nickel wire electrically with a constant power and recording the temperature of the wire, as deduced from its resistance, as a function of time. Bäckstrom and Chaussy[91] modified this method by investigating C_p and the λ_{ij} tensor: the specimen is ground flat and the boundary plane is oriented parallel to two principal axes of the conductivity tensor. Two parallel metal strips in one of the main directions are evaporated onto this surface. One of the strips is heated with a constant d.c. power, the other is used as an a.c.-driven thermometer. In thermally anisotropic samples, two parameters of the type λ_{11} λ_{33} and ρ C_p (ρ, density) are obtained. In consequence, additional studies with the metal strips deposited in the other principal axis enable λ_{11}, λ_{22}, λ_{33} and C_p to be measured.

6. SPECIAL APPLICATIONS

The reviewed non-adiabatic procedures represent a particularly useful tool to study heat capacities in the presence of extreme or unusual conditions at high pressure, extremely low temperatures, radioactive samples, etc.

6.1 High pressures

Many attempts to achieve comparatively accurate data of specific heat of pressurized samples have met with considerable difficulties in the past. Progress in this area has been hampered by the lack of attractive experimental methods. Previous studies have either used adiabatic calorimetry[25, 26], differential techniques[27], such as differential thermal analysis or differential scanning calorimetry (DSC). Conventional measurement of the total heat capacity of sample and high pressure cell, using adiabatic calorimetry yields accuracies of only a few percent, since the heat capacity of the sample is small relative to that of the cell and the addenda heat capacity usually amounts to 90% or more of the total. In the DSC approach, there are problems in the choice of the reference and difficulties arise from the relatively rapid rate at which the sample temperature changes.

Recently, the transient methods (measurement of λ and C_p) and a.c. calorimetry opened up new promising ways for further developments: previous attempts in this field are briefly reviewed by Jura and Stark[93]. The most successful method yet published seems to be the work of Anderson and Bäckstrom[92], in which the thermal diffusivity $D = \lambda/C_p$ is determined by measurement of the phase shift and attenuation of a cylindrical heat wave superimposed on a steady, radial heat flow under pressures of 100 kilobar. λ is determined by a standard procedure. The requirement of large samples limits the method to rather low pressures. Loriers-Susse et al.[28] describe a pulse-heating (heat pulses $\simeq$ 100 μsec) technique which has several advantages over

that of Jura and Stark[93]. The sensitivity is increased to 0.1 %. Baloga and Garland[24] adapted a.c. calorimetry for use at hydrostatic pressures up to 3 kb, but there seems no hindrance to going to higher pressures. The theoretical background of the technique is extended and discussed.

6.2 Extremely low temperatures

The development of the a.c. technique and relaxation time have led to considerable progress in very low-temperature calorimetry ($T < 1$ K), both methods have been applied[44, 82, 94]. The related basic problems are vibrational heating (see Sect. 5.1), detection and stabilization of extremely low thermometer current and voltages (nanoAmperes and μV), and small heating energies (milliergs!), good thermal coupling between sample, thermometer and heater as well as evaluation of external and internal relaxation times and their temperature dependence. Several experimental runs are necessary to find out the optimized heat link parameters, best thermometer or the required τ values.

Adiabatic calorimetry at temperatures below 100 mK suffers also from heat-leak problems, and is, in fact, not adiabatic but rather quasi-adiabatic. The sample heat capacity gets smaller and smaller in comparison with the heat leak if the temperature is decreased. The heat leak is no longer a small perturbation and conventional extrapolation analysis techniques must be replaced by non-adiabatic curve fitting. The transition from strong adiabatic measurements ($\tau_e \simeq \infty$) to relaxation time measurements is continuous ($\tau_e \simeq$ sec). Usually intermediate conditions ($\tau_e \simeq$ min) are given in the case of adiabatic calorimetry below 0.3 K; then simply a rapid recording of temperature vs. time[94] or logarithmic extrapolation of the final temperature from the drift temperature is applied. The very different techniques employed to match the experimental curves and to extrapolate ΔT for calculation of C_p have been discussed by several groups; a detailed discussion would exceed the frame of this contribution[95–98].

In addition, cryogenic problems multiply below 0.3 K. Several of the problems have been discussed at the end of Sect. 5.1. Surveys on the special techniques of very low temperatures are given in ref. 61.

6.3 Other calorimetric measurements

The determination of heat capacities on samples of low thermal diffusivity or powders requires special techniques as "dilution" of high thermal conductivity material among the sample or the distribution of the sample onto copper fans[13, 100] or other special arrangements are used[101]. A long time, highly constant stabilization of shield temperature is required. Samples with intrinsic radioactivity have been best measured by heat-leak methods[33].

7. CONCLUSION AND OUTLOOK

Significant advances have been accomplished since the time of Nernst to ease the burden of experimentalists in this field. Automation by application of computers

and the developemnt of non-adiabatic techniques are the highlights of the last decade.

Automation does not reduce the time necessary for measurement. However, final results, which before might have taken several days to be computed, can now be obtained immediately during the experiment. But precautions must, of course, be taken to ensure that information is not lost during data processing and that rigorous and repeated tests are included in the entire experimental procedure.

The non-adiabatic methods permit high-precision measurements on samples of less than 1 mg also in the temperature range below 1 K; these techniques have considerably extended the possibility of studying expensive and rare materials.

High-performance electronic circuits, control of the shield temperature with an accuracy of micro-degrees lead to an overall improved precision of the data, showing an experimental error of only 0.1–0.5%. Today, a significant increase in precision beyond this point does not seem to be required for most current problems. The design of calorimeters seems to be nearly perfect. Nevertheless, there are still several problems left that have to be solved.

There is the common demand for improvement in the design and calorimeter technique for more rapid and secure loading of materials into calorimeters, especially such substances which must not be exposed to the atmosphere.

There is the need for much more experience and knowledge, theoretical background, and perhaps for new technological innovations, to investigate the specific heat of samples in the presence of high pressures and at very low temperatures.

There remains the problem of thermometry. Very small, reproducible thermometers of extremely small heat capacities are still needed. Thermometry under high pressure or high magnetic fields has not yet reached the high standard of technical perfection, as reached, for example, in conventional Nernst calorimetry.

Finally, the rather well-developed, commercially available differential-scanning-calorimeters can still be improved and will probably extend their field of application to lower and lower temperatures.

ACKNOWLEDGEMENTS

I want to thank P. Rödhammer, J. Haag and P. de la Cruz for their fruitful collaboration. It is a pleasure for me to thank H. Grundel, P. Martin and H. v. Schickfus for several valuable and stimulating discussions and for critically reading the manuscript. The assistance of K. Ripka in carrying out several measurements is gratefully acknowledged.

REFERENCES

1 W. Gaede, *Z. Phys.*, 4 (1902) 105.
2 W. Nernst, *Sitzungsber. K. Preuss. Akad. Wiss.*, 12 (1910) 261.
3 A. Eucken, *Z. Phys.*, 10 (1909) 586.
4 W. H. Keesom and J. N. van den Ende, *Commun. Kamerlingh Onnes Lab. Univ. Leiden*, 219B (1932) 2196.
5 J. C. Southard and D. H. Andrews, *J. Franklin Inst.*, 209 (1930) 349.

6 A. G. Cole, J. O. Hutchens, R. A. Robie and J. W. Stout, *J. Am. Chem. Soc.*, 82 (1960) 4807. R. W. Hill, Low Temperature Calorimetry in K. Mendelssohn (Ed.), *Progress in Cryogenics*, Vol. 1, Heywood, London, 1959. P. H. Keesom and N. Pearlmann, *Handbuch der Physik*, Vol. XIV (I), Springer, Heidelberg, 1956, p. 282.

7 E. F. Westrum, G. T. Furukawa and J. P. McCullough, in J. P. McCullough and D. W. Scott (Eds.), *Experimental Thermodynamics*, Vol. I, Butterworth, London, 1968, p. 133 (Review).

8 D. E. Moody and P. Rhodes, *Cryogenics*, 3 (1963) 77.

9 H. J. Blythe, T. J. Harvey, F. E. Hoare and D. E. Moody, *Cryogenics*, 4 (1964) 28.

10 Th. G. Kollie, *Rev. Sci. Instrum.*, 38 (1967) 1452.

11 D. L. Martin and R. L. Snowdon, *Rev. Sci. Instrum.*, 41 (1970) 1869.

12 J. Pinel and C. Lebeau, *J. Phys.*, 5 (1972) 688.

13 V. Novotny and P. P. M. Meincke, *Rev. Sci. Instrum.*, 44 (1973) 817.

14 C. Shin and C. M. Criss, *Rev. Sci. Instrum.*, 46 (1975) 1043.

15 D. L. Martin, L. L. T. Bradley, W. J. Cazimir and R. L. Snowdon, *Rev. Sci. Instrum.*, 44 (1973) 675. D. L. Martin, *Rev. Sci. Instrum.*, 46 (1975) 1670.

16 R. E. Schwall, R. E. Howard and G. R. Stewart, *Rev. Sci. Instrum.*, 46 (1975) 1054.

17 O. Joseph, D. E. Moody and J. P. Whitehead, *J. Phys. E*, 9 (1976) 595.

18 D. Moses, O. Ben-Aroya and N. Lupu, *Rev. Sci. Instrum.*, 48 (1977) 1098.

19 E. Gmelin and P. Rödhammer, *J. Phys. E*, to be published.

20 P. F. Sullivan and G. Seidel, *Phys. Lett.*, 25 (1967) 229; *Phys. Rev.*, 173 (1968) 679.

21 R. Bachmann, F. J. di Salvo, Jr., T. H. Geballe, R. L. Greene, R. E. Howard, C. N. King, H. C. Kirsch, K. N. Lee, R. E. Schwall, H. U. Thomas and R. B. Zubeck, *Rev. Sci. Instrum.*, 43 (1972) 205.

22 W. N. Lawless and L. G. Rubin, *Rev. Sci. Instrum.*, 42 (1971) 561. D. Bakalyar, R. Swinehart, W. Weyhmann and W. N. Lawless, *Rev. Sci. Instrum.*, 43 (1972) 1221. J. B. Hartmann and T. F. McNelly, *Rev. Sci. Instrum.*, 48 (1977) 1072.

23 Several references in which further communications are indicated: L. J. Neuringer, A. J. Perlmann, L. G. Rubin and Y. Shapira, *Rev. Sci. Instrum.*, 40 (1969) 1314; *Rev. Sci. Instrum.*, 42 (1971) 9. H. H. Sample and L. J. Neuringer, *Rev. Sci. Instrum.*, 45 (1974) 1389. A. von Middendorff, *Cryogenics*, 11 (1971) 318. T. Knittel, *Cryogenics*, 13 (1973) 370. J. Sanchez, A. Benoit and J. Floquet, *Rev. Sci. Instrum.*, 48 (1977) 1072. H. Alms, R. Tillmanns and S. Roth, *Rev. Sci. Instrum.*, 49 (1978).

24 J. D. Baloga and C. W. Garland, *Rev. Sci. Instrum.*, 48 (1977) 105.

25 E. B. Amitin, Y. A. Kovalevskoya and I. E. Paukov, *Sov. Phys.-Solid State*, 14 (1973) 2902. D. B. McWhan, J. P. Remeika, S. D. Bader, B. B. Triplett and N. E. Philips, *Phys. Rev. B*, 7 (1973) 3079.

26 S. D. Bader, N. E. Philips and D. B. McWhan, *Phys. Rev. B*, 7 (1973) 3079, 4686.

27 N. J. Trappeniers and Th. J. van den Molen, *Physica*, 32 (1966) 1161. R. Shashidhar and S. Chandrasekhar, *J. Phys.*, 36 (1975) C1.

28 C. Loriers-Susse, J. P. Bastide and G. Bäckström, *Rev. Sci. Instrum.*, 44 (1973) 1344.

29 P. Anderson and G. Bäckström, *High Temp.-High Pressures*, 4 (1972) 101 and refs. therein.

30 G. Jura and W. A. Stark, *Rev. Sci. Instrum.*, 40 (1969) 656.

31 A. Cezairliyan, *High Temp.-High Pressures*, 1 (1969) 517 (review).

32 P. Pruzan, L. T. Minassian, P. Figuiere and H. Szwarc, *Rev. Sci. Instrum.*, 47 (1976) 66.

33 R. J. Trainor, G. S. Knapp, M. B. Brodsky, G. J. Pokorny and R. B. Snyder, *Rev. Sci. Instrum.*, 46 (1975) 1368. C. W. Dempesy, J. E. Gordon and R. H. Romer, *Phys. Rev. Lett.*, 11 (1963) 547. R. A. O. Hall, J. A. Lee, M. J. Mortimer and P. W. Sutcliffe, *Cryogenics*, 15 (1975) 129.

34 K. Eiermann, R. Hoffmann and W. Knappe, *Kolloid Z. Z. Polym.*, 250 (1972) 111.

35 H. Steffen and H. Wollenberger, *Rev. Sci. Instrum.*, 44 (1973) 937.

36 L. G. Rubin, *Cryogenics*, 10 (1970) 14 (Review).

37 C. A. Swenson, *Crit. Rev. Solid State Phys.*, 1 (1971) 1 (review).

38 E. S. R. Gopal, *Specific Heats at Low Temperatures*, Plenum Press, New York, 1966 (review).

39 D. C. Ginnings and G. T. Furukawa, *J. Am. Chem. Soc.*, 75 (1953) 522, 5359.

40 D. W. Osborne, H. E. Flotow and F. Schreiner, *Rev. Sci. Instrum.*, 38 (1967) 159.

41 J. Haag and E. Gmelin, to be published.

42 A. Sommerfeld, *Z. Phys.*, 47 (1928) 1.

43 U. Rindelhart and E. Hegenbarth, *Wiss. Z. Tech. Univ. Dresden*, 25 (1976) 761.

44 F. de la Cruz and E. Gmelin, unpublished results.
45 P. Rödhammer, E. Gmelin and W. Weber, *Solid State Commun.*, 16 (1975) 1205.
46 P. Rödhammer, E. Gmelin, W. Weber and J. P. Remeika, *Phys. Rev.*, 15 (1977) 711. P. Rödhammer, W. Weber, E. Gmelin and K. H. Rieder, *J. Chem. Phys.*, 64 (1976) 581.
47 W. K. Robinson and S. A. Friedberg, *Phys. Rev.*, 117 (1960) 402.
48 J. W. Stout and W. B. Hardley, *J. Chem. Phys.*, 40 (1964) 55.
49 R. Georges, E. Gmelin, D. Landau and J. C. Lasjaunias, *C.R. Acad. Sci. Paris*, 269 (1969) 827.
50 E. Gmelin, unpublished result.
51 These cryogenic problems are discussed in the following text books: G. K. White, *Experimental Techniques in Low Temperature Physics*, Oxford University Press, 1967. A. C. Rose-Innes, *Low Temperature Techniques*, English University Press, London, 1964. Also see refs. 6 and 7.
52 E. Gmelin, *Cryogenics*, 7 (1967) 225.
53 W. H. Keesom and J. A. Kok, *Physica*, 1 (1934) 770.
54 E. F. Westrum, Jr., J. B. Hatcher and D. W. Osborne, *J. Chem. Phys.*, 21 (1953) 419.
55 K. G. Ramanathan and T. M. Srinivasan, *Philos. Mag.*, 46 (1956) 338.
56 J. A. Rayne, *Aust. J. Phys.*, 9 (1956) 189.
57 F. J. Webb and J. Wilks, *Proc. R. Soc. London, Ser. A*, 230 (1955) 549. W. Hill and P. L. Smith, *Philos. Mag.*, 44 (1953) 636.
58 E. M. Forgan, *Cryogenics*, 14 (1974) 207.
59 Most descriptions of calorimeters included detailed information on the radiation shield temperature stabilization, as refs. 10, 11, 15, 18, 19, 52, 65.
60 E. D. West and S. Ihihara, *Rev. Sci. Instrum.*, 40 (1969) 1356 and refs. therein.
61 The techniques and related problems arising by embarking onto the millikelvin region have been reviewed by: O. V. Lounasmaa, *Experimental Principles and Methods Below* 1 K, Academic Press, London, 1974. W. J. Huiskamp and O. V. Lounasmaa, *Rep. Prog. Phys.*, 36 (1973) 423 (review)
62 R. P. Hudson, H. Marsmak, R. J. Soulen and D. B. Utton, *J. Low Temp. Phys.*, 20 (1975) 1 (review).
63 R. C. Richardson, *Physica B*, 90 (1977) 47.
64 D. S. Parker and L. R. Coruccini, *Cryogenics*, 15 (1975) 499.
65 The following lists a selection of papers, wherein further references are given: D. L. Martin, *Proc. Phys. Soc.*, 83 (1963) 99. T. Shinoda, H. Chihara and S. Seki, *J. Phys. Soc. Jpn.*, 19 (1964) 1637. M. Dixon, F. E. Hoare, T. M. Holden and D. E. Moody, *Proc. R. Soc. London, Ser. A*, 285 (1965) 561. D. W. Osborne, F. Schreier, M. E. Flotow and J. G. Malm, *J. Chem. Phys.*, 57 (1972) 3401. J. Bousquet, M. Prost and M. Diot, *J. Chim. Phys.*, 6 (1972) 1004. P. A. O'Hare and H. R. J. Hoekstra, *J. Chem. Thermodyn.*, 5 (1973) 769.
66 B. Gliss, *Comput. Phys. Commun.*, 15 (1978).
67 Emmerson and Cumings, Comp., Canton, Massachusetts, U.S.A.
68 J. K. Logan, J. R. Clement and H. R. Jeffer, *Phys. Rev.*, 105 (1957) 1435.
69 H. Gobrecht, J. J. Veyssie and L. Weil, *Ann. Acad. Sci. Fenn.*, 210 (1966) 40. P. R. Roach, J. B. Ketterson, B. M. Abraham and J. Monson, *Rev. Sci. Instrum.*, 42 (1975) 207.
70 M. Hafendörfer, private communication. The constant current source has been designed in the electronic workshop of the Institute.
71 J. F. Cochran, C. A. Schiffmann and J. E. Neighbor, *Rev. Sci. Instrum.*, 37 (1966) 499 and refs. therein.
72 T. Ashworth and H. Steeple, *Cryogenics*, 8 (1968) 225. D. L. Martin and R. L. Snowdon, *Can. J. Phys.*, 44 (1966) 1449. G. Pompe and E. Hegenbarth, *Cryogenics*, 8 (1968) 309.
73 W. W. White, H. J. Song, J. I. Rives and D. P. Landau, *Phys. Rev.*, 4 (1971) 4605; *Conf. on Phase Transitions and their Applications, University Park, Pasadena, U.S.A. 23–25 May 1973*, Pergamon, New York, 1973, p. 253.
74 K. Naito, N. Kamegashira, N. Yamada and J. Kitagawa, *J. Phys. E*, 6 (1973) 836 and refs. therein.
75 R. Lagnier, J. Pierre and M. J. Mortimer, *Cryogenics*, 17 (1977) 349.
76 Mettler Instrumente A.G., CH 8606 Greifensee-Zürich, Schweiz. M.V.E. Electronique Avion, 8 impasse, Toulouse, F-78 Versailles, France. Perkin-Elmer, Corp. Norwalk, California, U.S.A. Setaram, 101 rue de Seze, F-69451 Lyon, Cedex 3, France.

77 R. W. Jones, G. S. Knapp and B. W. Veal, *Rev. Sci. Instrum.*, 44 (1973) 807.
78 P. Marx, *Rev. Phys. Appl.*, 13 (1978) 298.
79 H. Grundel, P. de la Gruz and E. Gmelin, to be published.
80 Several representative references of authors using a.c. or relaxation-time techniques: D. L. Connelly, J. S. Loomis and D. E. Mapother, *Phys. Rev. B*, 3 (1971) 924. P. Manuel, H. Niedoba and J. J. Veyssie, *J. Phys. Appl.*, 7 (1972) 107. R. D. Hempstead and J. M. Mochel, *Phys. Rev. B*, 7 (1971) 924. A. A. Varchenko and Ya. A. Kraftmakher, *Phys. Status Solidi A*, 20 (1973) 387. J. Hatta and W. Rehwald, *J. Phys. C*, 10 (1977) 2075. G. Kämpf and W. Buckel, *Z. Phys. B*, 27 (1977) 315.
81 P. Handler, D. E. Mapother and M. Rayl, *Phys. Rev. Lett.*, 19 (1967) 356.
82 R. J. Schutz, *Rev. Sci. Instrum.*, 45 (1974) 548.
83 T. S. Chen and F. W. de Wette, *Phys. Rev.*, 17 (1978) 835 and references therein.
84 G. D. Zally and J. M. Mochel, *Phys. Rev. B*, 6 (1972) 4142. B. Dodson, T. Low and J. Mochel, *Rev. Sci. Instrum.*, 48 (1977) 290. K. Noto, N. Kobayashi and Y. Muto, *Jpn. J. Appl. Phys.*, 15 (1976) 2449.
85 N. V. Zavaritsky, in K. Mendelssohn (Ed.), *Progress in Cryogenics*, Vol. 1, Heywood, London, 1959, p. 209.
86 B. Bertram, D. C. Heberlein, D. J. Sandiford, L. Shen and R. R. Wagner, *Cryogenics*, 10 (1970) 326. Y. Kogure and Y. Hiki, *Jpn. J. Appl. Phys.*, 12 (1973) 814.
87 R. L. Filler, P. Lindenfeld and G. Deutscher, *Rev. Sci. Instrum.*, 46 (1975) 439.
88 M. Gershenson and S. Alterovitz, unpublished calculations.
89 H. Gobrecht, H. Nelkowski, W. Seifert and R. Krüger, *Waerme Stoffuebertrag.*, 3 (1970) 96.
90 O. Sandberger, P. Anderson and P. Bäckström, *J. Phys. E*, 10 (1977) 474.
91 G. Bäckstrom and J. Chaussy, *J. Phys. E*, 10 (1977) 767.
92 P. Anderson and P. Bäckstrom, *High Temp.-High Pressures*, 4 (1972) 101.
93 G. Jura and W. A. Stark, *Rev. Sci. Instrum.*, 40 (1969) 656.
94 G. J. Sellers and A. C. Anderson, *Rev. Sci. Instrum.*, 45 (1974) 1256.
95 P. Costa-Ribeiro, B. Picot, J. Souletie and D. Thoulouze, *Rev. Phys. Appl.*, 9 (1974) 749.
96 H. K. Collan, T. Hekkilä, M. Krusius and G. R. Pickett, *Cryogenics*, 10 (1970) 389.
97 J. C. Lasjaunias, B. Picot, A. Ravex, D. Thoulouze and M. Vandorpe, *Cryogenics*, 17 (1977) 111.
98 W. J. Huiskamp and G. Reedijk, *Physica B*, 83 (1976) 85.
100 D. L. Johnson, D. H. Cluxton and R. A. Young, *Rev. Sci. Instrum.*, 44 (1973) 16.
101 J. Baturic-Rubcic, D. Durek and A. Rubcic, *J. Phys. E*, 9 (1976) 373.
102 H. M. Haendler, D. Mootz, A. Rabenau and G. Rosenstein, *J. Solid State Chem.*, 10 (1974) 175.
103 C. Schmidt and E. Gmelin, *Solid State Commun.*, 21 (1977) 987.